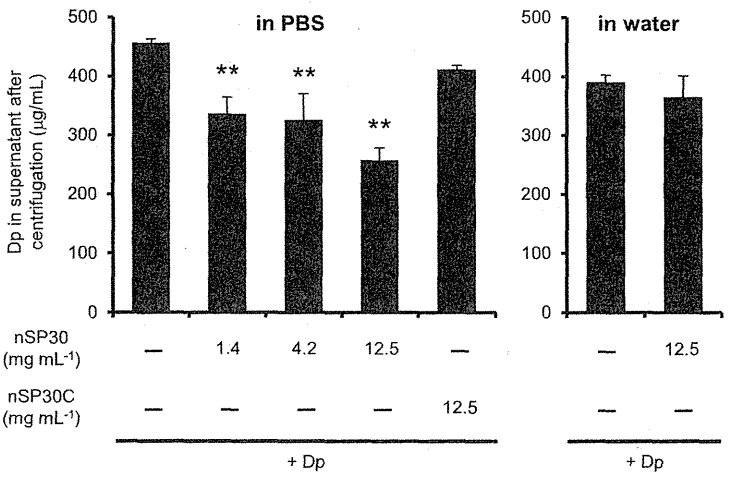

Fig. 8 Evaluation of absorption of Dp to nSP30. The amount of Dp in the supernatant of each centrifuged sample was determined (OD_{280}). Data are given as means ± SD ($n = 3$). $^{**}P < 0.01$ vs. Dp-alone

these observations suggest that the IgE-biased immune response in the current study was not solely due to the low Dp exposure resulting from the agglomeration of Dp and nSP30. Perhaps the agglomerates of Dp and nSP30 in PBS not only decreased the Dp exposure dose but also behaved as a 'depot,' thus controlling the allergen concentration, prolonging allergen exposure, and subsequently causing IgE-biased allergic sensitization. We believe additional studies that focus on the effect of nanoparticles on allergen penetration kinetics in the skin would be beneficial to confirm the safety of cutaneous exposure to nanomaterials. However, we acknowledge the need for additional studies in which the exposure scenario is more representative of that in humans to define the safety of concurrent cutaneous exposure to nanomaterials and allergen.

It is well recognized that there are some situations in our daily lives, the development of atopic allergy is inhibited by higher dose exposure to allergen due to high induction of blocking IgG [46–48]. Particularly in these high-dose exposure situations, we suggest that allergen-nanoparticle agglomerates, by inducing IgE-biased immune responses, might play a critical role in the development of atopic allergy. In addition, the IgE-biased immune response induced by cutaneous exposure to agglomerates of allergen and nanoparticles in our mice was similar to those humans with atopic allergies, who often have a low IgG/IgE ratio, as mentioned earlier [40, 41]. Therefore epidemiologic studies that address cutaneous as well as inhalational exposure to nanomaterials may improve our understanding of the onset of atopic allergy.

Recently, Ilves M. *et al.* described the effects of cutaneous exposure to nano-sized ZnO (nZnO) administered with model antigens, ovalbumin and staphylococcal enterotoxin B, on AD-like skin lesions and antibody responses [49]. Interestingly, the effects observed for nZnO and an antigen were similar to the effects of agglomerates of Dp and nSP30: nZnO suppressed allergen-induced skin inflammation and induced low-level IgG production in the context of a high IgE response. The authors of the previous study [49] did not address changes of nZnO dispersibility by mixing allergen, but considering that nZnO is predisposed to forming agglomerates and might adsorb a coexisting substance [50], nZnO might play similar role to that of nSP30. To better understand the hazards of nanomaterials so that we can maximize their potential benefits, we should pay increased attention to the state of nanoparticles (*e.g.* dispersibility) in administration in nanotoxicology studies. We consider this focus particularly applicable in the hazard evaluation of nanomaterials that are in the presence of other substances, which could interact with them.

Cutaneous exposure to aggregates or agglomerates of nanomaterials is generally considered to be safer than is similar exposure to individual nanoparticles, mainly because agglomerates of nanomaterials have difficulty penetrating the skin [50]. However, Dp and nSP30 induced an IgE-biased immune response only when they formed agglomerates. Although these results represent only indirect effects of nanomaterials, we think that hazard identification is necessary even when nanomaterials are considered to be unable to cross the skin barrier (*e.g.* when nanomaterials form aggregates or agglomerates). In contrast, surface modification of the nSP30 with carboxyl groups suppressed the adsorption of the allergen and did not induce IgE-biased allergic sensitization (Fig. 6). An increased understanding of the regulatory factors that

induce the agglomeration of silica nanoparticles is crucial for appropriate regulation of the surface properties of nanomaterials so that they can be used safely.

Conclusions

Cutaneous exposure to agglomerates of Dp and nSP30 induced an IgE-biased immune response in NC/Nga mice and increased their sensitivity to anaphylaxis. Surprisingly, these results were independent of the innate biologic effects of nSP30; these results required both simultaneous exposure to Dp and nSP30 and their agglomeration. In particular, features of the mice with IgE-biased immune response induced by cutaneous exposure to agglomerates of allergen and nanoparticles resembled those of humans with atopic allergies, who often have a low IgG/IgE ratio; follow-up epidemiologic studies that focus cutaneous compared with inhalational exposure to nanomaterials might improve our understanding of the onset of atopic allergy. In light of our findings, we suggest that minimizing the interaction between nanomaterials and allergens may improve the safety of topically applied products containing nanomaterials.

Methods

Silica nanoparticles

nSP30 and nSP30C (nSP30C is a surface modified nSP30 with carboxyl groups) silica nanoparticles (diameter, 30 mm) were purchased from Micromod Partikeltechnologie (Rostock/Warnemünde, Germany). Suspensions of silica nanoparticles were stored at room temperature. Immediately prior to use, the suspensions were sonicated at 400 W for 5 min at 25 °C and then vortexed for 1 min.

Mice

Female NC/Nga slc mice were purchased from SLC (Kyoto, Japan) and used at 6 wk of age. All animal experiments were performed in accordance with the institutional guidelines of Osaka University and National Institute of Biomedical Innovation regarding the ethical treatment of animals.

Preparation of the mixtures of Dp and nSP30s

To prepare the mixtures of nSP30s and Dp (Cosmo Bio LSL, Tokyo, Japan), we first combined nSP30s (25 mg mL^{-1} in water) and concentrated PBS (1.1× to 4.6×; the concentration of the PBS stock used depended on the concentration of nSP30s needed in the final sample, the diluent for which was 1× PBS). We then added the stock solution of Dp (2.78 mg protein mL^{-1} in PBS) to the solutions containing various concentrations of nSP30s. As soon as the nSP30s and Dp solutions were combined, the mixtures were vortexed for 1 min, allowed to incubate at room temperature for 0.5 to 1.5 h, and vortexed again for 1 min just prior to use.

Physicochemical examination of silica nanoparticles

TEM (H-7650; Hitachi High-Technologies Corporation, Tokyo, Japan) was used to assess the size and shape of the silica nanoparticles. nSP30 and nSP30C nanoparticles were diluted to 0.25 mg mL^{-1} in PBS or deionized water, and the mean particle diameter and zeta potential at 25 °C were measured by using a Zetasizer Nano ZS (Malvern Instruments, Worcestershire, UK). Specifically, the mean diameters and particle size distributions of the nanoparticles were measured by means of a dynamic light-scattering method, whereas zeta potentials were measured by laser Doppler electrophoresis; both types of measurements were performed by using capillary cells (Malvern Instruments). The pH of each particle suspension was measured by using an ISFET pH meter (Shindengen, Tokyo, Japan).

Skin painting and assessment of allergic response

Using a hair-removal cream (Epilat; Kracie, Tokyo, Japan), we removed the hair from the backs of all mice twice during each experiment (on day 1 and on day 18–20). Mice were treated either with Dp (1 mg mL^{-1} fin. conc) alone or with silica nanoparticles (nSP30 or nSP30C, 12.5 mg mL^{-1} fin. conc.) in 120 μL PBS by painting the ventral side of both ears and the depiliated dorsum (20 μL per ear and 80 μL on the back) on alternate days or every third day for 4 wk for a total of 13 applications. Additional mice were painted with Dp only on one day followed by painting with nSP30 alone on the next day; this alternating pattern was repeated for a total of 13 applications of each solution over 4 wk. Regardless of the dose schedule used, any sample remaining from a previous application was removed by gently wiping with a disposable wipe (Kim wipes, Crecia, Tokyo, Japan) wetted with 70 % ethanol.

We used a dial thickness gauge (0.001-mm type; Ozaki Manufacturing, Tokyo, Japan) to measure ear thickness weekly. To evaluate the severity of the IgE-mediated allergic response' instead, we used a systemic anaphylaxis model. Specifically, at 1 wk after the final skin painting, each mouse was challenged with an intravenous injection of Dp (15 μg in 200 μL PBS). The severity of anaphylactic shock was assessed according to the change in rectal temperature measured by using a digital thermometer (KN-91; Natsume Seisakusho, Tokyo, Japan).

Histologic analysis

At 24 h after the final topical treatment, the ears of euthanized mice were removed, placed in fixative solution (4 % paraformaldehyde in PBS; Wako, Osaka, Japan), embedded in paraffin, and sectioned. The tissue sections were stained with hematoxylin and eosin or with toluidine blue. Histopathological examination was performed by the Applied Medical Research Laboratory (Osaka,

Japan). For each sample, representative symptoms of AD (scab formation, acanthosis and inflammatory cell infiltration) were scored as follows: 0, none; 1, slight; 2, mild; 3, moderate; and 4, severe. In addition, we counted the number of mast cells in 3 random high-power fields (magnification, 400×).

Blood sampling

Using hematocrit capillary tubes (Terumo, Tokyo, Japan), we obtained blood samples from the retro-orbital venous plexus once each week during the study period. At 24 h after the final skin painting, blood was collected by cardiocentesis into heparin-treated syringes and centrifuged at 3000 × *g* at 4 °C; the resulting plasma was stored at −80 °C until analysis.

Quantitation of total IgE concentration

The total IgE concentration in plasma was measured by using an ELISA kit (BD Biosciences, San Diego, CA, USA) according to the manufacturer's instructions.

Detection of Dp-specific antibody

The levels of Dp-specific antibody in plasma were determined by ELISA. To detect IgG, IgG1, IgG2a, IgG2b and IgG3, we coated ELISA plates (Maxisorp, type 96 F; Nunc A/S, Roskilde, Denmark) with Dp in PBS (50 μg mL^{-1}). The coated plates were incubated with 2 % Block Ace (Dainippon Sumitomo Pharmaceuticals, Osaka, Japan). Plasma samples were diluted by 2 % Block Ace and these dilutions were added to the Dp-coated plates. After incubation with plasma, the coated plates were incubated with a horseradish peroxidase–conjugated goat anti-mouse IgG, IgG1, IgG2a, IgG2b or IgG3 solution (SouthernBiotech, Birmingham, AL, USA) for two hours at room temperature. After the incubation, the color reaction was developed with tetramethyl benzidine (Moss, Inc.; Pasadena, MD, USA), stopped with 2 N H_2SO_4, and measured at $OD_{450-620}$ on a microplate reader.

To detect Dp-specific IgE, we coated ELISA plates (Maxisorp, type 96 F) with purified rat anti-mouse IgE (2 μg mL^{-1}; R35-72, BD Biosciences;), incubated them with Block Ace, and added samples of diluted plasma as described earlier. Treated plates were incubated with biotin-conjugated Dp (5 μg mL^{-1}) followed by horseradish peroxidase–coupled streptavidin (Southern Biotechnology Associates). Color detection was performed as described earlier.

Isolation of splenocytes

Spleens were removed aseptically and placed in RPMI 1640 (Wako) supplemented with 10 % fetal bovine serum, 10 mL L^{-1} of a 100× nonessential amino acid solution (Gibco, Invitrogen, Carlsbad, CA, USA), 50 μM 2-mercaptoethanol (Gibco), and 1 % antibiotic cocktail (10,000 U mL^{-1} penicillin, 10,000 μg mL^{-1} streptomycin, 25 μg mL^{-1} amphotericin B; Gibco). Single-cell suspensions of splenocytes were treated with ammonium chloride to lyse the red blood cells; treated splenocytes then were washed, counted, and suspended in RPMI 1640.

Cytokine assays

To determine antigen-specific cytokine (IFN-γ and IL-4) responses, splenocytes (5×10^5 cells $well^{-1}$) were stimulated with Dp antigen (100 μg mL^{-1}) *in vitro*. After 24 h incubation at 37 °C (95 % room air, 5 % CO2), stimulated splenocytes were washed, and the numbers of IFN-γ- and IL-4-producing cells were determined by using an ELISPOT assay kit (BD Biosciences) according to the manufacturer's instructions.

Measurement of amount of Dp adsorbed to silica nanoparticles

Solutions of Dp (1 mg mL^{-1} fin. conc.) + each nSP immediately after preparation in PBS or water for 30 min at 25 °C were centrifuged (2 h, 40,000 × *g*, 4 °C). The amount of Dp in the supernatant then was determined spectrophotometrically (OD_{280}; Nanodrop 2000, Thermo Scientific, Kanagawa, Japan).

Statistical analysis

Statistical analyses were performed with Ekuseru-Toukei 2010 software (Social Survey Research Information Co., Ltd., Tokyo, Japan). All data are presented as means ± SEMs. Significant differences between control groups and experimental groups were determined by using the Dunnett test; a *P* value less than 0.05 was considered significant.

Methods for additional files are available in (Additional file 5).

Additional files

Additional file 1: Effects of nSP30 nanoparticles alone on skin. (A) Effect of topical treatment with nSP30 alone on ear thickness in NC/Nga mice. (B, C) Histology of ear sections stained with (B) hematoxylin and eosin (HE) or (C) toluidine blue (TB). Scale bar, 50 μm. (D) Scores for several symptoms characteristics of AD as evaluated in HE-stained sections. (E) Mast cell infiltration evaluated in TB-stained as the number of mast cells per high-power (*i.e.*, 400×) field. (F) Total IgE concentration at 24 h after the final treatment. N. D., not detected (<30 ng mL-1). Data are given as mean ± SEMs (n = 5).

Additional file 2: Dose-dependence of the effects of nSP30 nanoparticles on mite-allergen (Dp)-specific antibody responses. A-C, Plasma levels of Dp-specific (A) IgE, (B) IgG, and (C) IgG subtypes in plasma collected from NC/Nga mice after topical treatment with Dp alone or with 1.4, 4.2, or 12.5 mg mL-1 nSP30 (as analyzed by ELISA). Data are given as mean ± SEMs (n = 5). *$P < 0.05$. **$P < 0.01$ vs. Dp-alone group.

Additional file 3: Effects of nSP30 nanoparticles on effector cytokines induced by mite allergen (Dp). Levels of Dp-specific effector cytokines in the supernatants of NC/Nga mouse splenocytes stimulated with 100 μg mL-1 Dp for 4 days (determined by use of cytokines

immunoassay or ELISA). Data are given as means ± SEMs (n = 5). *P < 0.05. **P < 0.01 vs. Dp-alone group.

Additional file 4: Effects of administration route of mite allergen (Dp) + nSP30 mamoparticles on Dp-sepcific antibody response. Levels of Dp-specific IgE and IgG in plasma collected from NC/Nga mice after treatment with Dp alone or Dp + nSP30 by intradermal (foot-pad injection), intranasal, or oral administration (as analyzed by ELISA). Data are given as means ± SEMs (n = 3-6). **P < 0.01 vs. Dp-alone group.

Additional file 5: Additional methods.

Competing interests
The authors declare that they have no competing interests.

Authors' contributions
TH and YY designed the study; TH, HT, KI, AU, TM, and NN performed experiments; TH and YY collected and analyzed data; TH and YY wrote the manuscript; TYoshida, KN, HK, ST, TT, IKJ, HN, TYoshikawa, and KH provided technical support and conceptual advice. YT supervised all the projects. All authors discussed the results and commented on the manuscript. All authors read and approved the final mansucript.

Acknowledgements
This study was supported by Grants-in-Aid for Scientific Research from the Ministry of Education, Culture, Sports, Science and Technology of Japan (MEXT) and from the Japan Society for the Promotion of Science (JSPS); by a Grant-in-Aid for JSPS Fellows; by Health Labour Sciences Research Grants from the Ministry of Health, Labour and Welfare of Japan (MHLW); by The Takeda Science Foundation; by The Research Foundation for Pharmaceutical Sciences; by The Japan Food Chemical Research Foundation; by the Urakami Foundation; and by the Uehara Memorial Foundation.

Author details
[1]Laboratory of Toxicology and Safety Science, Graduate School of Pharmaceutical Sciences, Osaka University, 1-6 Yamadaoka, Suita, Osaka 565-0871, Japan. [2]Vaccine Creation Project, BIKEN Innovative Vaccine Research Alliance Laboratories, Research Institute for Microbial Diseases, Osaka University, 3-1 Yamadaoka, Suita, Osaka 565-0871, Japan. [3]BIKEN Center for Innovative Vaccine Research and Development, The Research Foundation for Microbial Diseases of Osaka University, 3-1 Yamadaoka, Suita, Osaka 565-0871, Japan. [4]Laboratory of Innovative Antibody Engineering and Design, Center for Drug Innovation and Screening, National Institute of Biomedical Innovation, 7-6-8 Saitoasagi, Ibaraki, Osaka 567-0085, Japan. [5]Laboratory of Biopharmaceutical Research, National Institute of Biomedical Innovation, 7-6-8 Saitoasagi, Ibaraki, Osaka 567-0085, Japan. [6]The Center for Advanced Medical Engineering and Informatics, Osaka University, 1-6 Yamadaoka, Suita, Osaka 565-0871, Japan. [7]Laboratory of Environmental Pharmacometrics, Graduate School of Pharmaceutical Sciences, Osaka University, 1-6 Yamadaoka, Suita, Osaka 565-0871, Japan. [8]Genome Information Research Center, Research Institute for Microbial Diseases, Osaka University, 3-1 Yamadaoka, Suita, Osaka 565-0871, Japan. [9]Laboratory of Adjuvant Innovation, National Institute of Biomedical Innovation, 7-6-8 Saitoasagi, Ibaraki, Osaka 567-0085, Japan. [10]Laboratory of Vaccine Science, Immunology Frontier Research Center, World Premier International Research Center, Osaka University, 3-1 Suita, Osaka 565-0871, Japan. [11]Division of Foods, National Institute of Health Sciences, 1-18-1 Kamiyoga, Setagaya-ku, Tokyo 158-8501, Japan.

Received: 18 April 2015 Accepted: 16 June 2015
Published online: 26 June 2015

References
1. Auffan M, Rose J, Bottero JY, Lowry GV, Jolivet JP, Wiesner MR. Towards a definition of inorganic nanoparticles from an environmental, health and safety perspective. Nat Nanotechnol. 2009;4(10):634–41. doi:10.1038/nnano.2009.242.
2. Cheng Z, Al Zaki A, Hui JZ, Muzykantov VR, Tsourkas A. Multifunctional nanoparticles: cost versus benefit of adding targeting and imaging capabilities. Science. 2012;338(6109):903–10. doi:10.1126/science.1226338.
3. Bowman DM, van Calster G, Friedrichs S. Nanomaterials and regulation of cosmetics. Nat Nanotechnol. 2010;5(2):92. doi:10.1038/nnano.2010.12.
4. Jain RK, Stylianopoulos T. Delivering nanomedicine to solid tumors. Nat Rev Clin Oncol. 2010;7(11):653–64. doi:10.1038/nrclinonc.2010.139.
5. Peters R, Kramer E, Oomen AG, Rivera ZE, Oegema G, Tromp PC, et al. Presence of nano-sized silica during *in vitro* digestion of foods containing silica as a food additive. ACS Nano. 2012;6(3):2441–51. doi:10.1021/nn204728k.
6. Yamashita K, Yoshioka Y, Higashisaka K, Mimura K, Morishita Y, Nozaki M, et al. Silica and titanium dioxide nanoparticles cause pregnancy complications in mice. Nat Nanotechnol. 2011;6(5):321–8. doi:10.1038/nnano.2011.41.
7. Setyawati MI, Tay CY, Chia SL, Goh SL, Fang W, Neo MJ, et al. Titanium dioxide nanomaterials cause endothelial cell leakiness by disrupting the homophilic interaction of VE-cadherin. Nat Commun. 2013;4:1673. doi:10.1038/ncomms2655.
8. Kulbok PA, Baldwin JH. From preventive health behavior to health promotion: advancing a positive construct of health. ANS Adv Nurs Sci. 1992;14(4):50–64.
9. Janssen NA, Brunekreef B, van Vliet P, Aarts F, Meliefste K, Harssema H, et al. The relationship between air pollution from heavy traffic and allergic sensitization, bronchial hyperresponsiveness, and respiratory symptoms in Dutch schoolchildren. Environ Health Perspect. 2003;111(12):1512–8.
10. Bartra J, Mullol J, del Cuvillo A, Davila I, Ferrer M, Jauregui I, et al. Air pollution and allergens. J Investig Allergol Clin Immunol. 2007;17 Suppl 2:3–8.
11. McCreanor J, Cullinan P, Nieuwenhuijsen MJ, Stewart-Evans J, Malliarou E, Jarup L, et al. Respiratory effects of exposure to diesel traffic in persons with asthma. N Engl J Med. 2007;357(23):2348–58.
12. Tsuji JS, Maynard AD, Howard PC, James JT, Lam CW, Warheit DB, et al. Research strategies for safety evaluation of nanomaterials, part IV: risk assessment of nanoparticles. Toxicol Sci. 2006;89(1):42–50.
13. Som C, Wick P, Krug H, Nowack B. Environmental and health effects of nanomaterials in nanotextiles and facade coatings. Environ Int. 2011;37(6):1131–42. doi:10.1016/j.envint.2011.02.013.
14. Rancan F, Gao Q, Graf C, Troppens S, Hadam S, Hackbarth S, et al. Skin penetration and cellular uptake of amorphous silica nanoparticles with variable size, surface functionalization, and colloidal stability. ACS Nano. 2012;6(8):6829–42. doi:10.1021/nn301622h.
15. Dhanirama D, Gronow J, Voulvoulis N. Cosmetics as a potential source of environmental contamination in the UK. Environ Technol. 2012;33(13–15):1597–608.
16. Li N, Xia T, Nel AE. The role of oxidative stress in ambient particulate matter-induced lung diseases and its implications in the toxicity of engineered nanoparticles. Free Radic Biol Med. 2008;44(9):1689–99. doi:10.1016/j.freeradbiomed.2008.01.028.
17. Matsuda H, Watanabe N, Geba GP, Sperl J, Tsudzuki M, Hiroi J, et al. Development of atopic dermatitis-like skin lesion with IgE hyperproduction in NC/Nga mice. Int Immunol. 1997;9(3):461–6.
18. Banerjee S, Resch Y, Chen KW, Swoboda I, Focke-Tejkl M, Blatt K, et al. Der p 11 is a major allergen for house dust mite-allergic patients suffering from atopic dermatitis. J Investig Dermatol. 2015;135(1):102–9. doi:10.1038/jid.2014.271.
19. Fuiano N, Diddi G, Delvecchio M, Cl C. Prevalence of positive atopy patch test in an unselected pediatric population. Clin Mol Allergy. 2015;13(1):2. doi:10.1186/s12948-015-0011-2.
20. Aioi A, Tonogaito H, Suto H, Hamada K, Ra CR, Ogawa H, et al. Impairment of skin barrier function in NC/Nga Tnd mice as a possible model for atopic dermatitis. Br J Dermatol. 2001;144(1):12–8.
21. Flohr C, Johansson SG, Wahlgren CF, Williams H. How atopic is atopic dermatitis? J Allergy Clin Immunol. 2004;114(1):150–8. doi:10.1016/j.jaci.2004.04.027.
22. Yagi R, Nagai H, Iigo Y, Akimoto T, Arai T, Kubo M. Development of atopic dermatitis-like skin lesions in STAT6-deficient NC/Nga mice. J Immunol. 2002;168(4):2020–7.
23. Coffman RL, Savelkoul HF, Lebman DA. Cytokine regulation of immunoglobulin isotype switching and expression. Semin Immunol. 1989;1(1):55–63.
24. Ozaki K, Spolski R, Feng CG, Qi CF, Cheng J, Sher A, et al. A critical role for IL-21 in regulating immunoglobulin production. Science. 2002;298(5598):1630–4. doi:10.1126/science.1077002.
25. Vogelzang A, McGuire HM, Yu D, Sprent J, Mackay CR, King C. A fundamental role for interleukin-21 in the generation of T follicular helper cells. Immunity. 2008;29(1):127–37. doi:10.1016/j.immuni.2008.06.001.

26. Palmer CN, Irvine AD, Terron-Kwiatkowski A, Zhao Y, Liao H, Lee SP, et al. Common loss-of-function variants of the epidermal barrier protein filaggrin are a major predisposing factor for atopic dermatitis. Nat Genet. 2006;38(4):441–6.
27. Weidinger S, O'Sullivan M, Illig T, Baurecht H, Depner M, Rodriguez E, et al. Filaggrin mutations, atopic eczema, hay fever, and asthma in children. J Allergy Clin Immunol. 2008;121(5):1203–9. doi:10.1016/j.jaci.2008.02.014. 5.
28. Lack G. Update on risk factors for food allergy. J Allergy Clin Immunol. 2012;129(5):1187–97. doi:10.1016/j.jaci.2012.02.036.
29. Hirai T, Yoshikawa T, Nabeshi H, Yoshida T, Tochigi S, Ichihashi K, et al. Amorphous silica nanoparticles size-dependently aggravate atopic dermatitis-like skin lesions following an intradermal injection. Part Fibre Toxicol. 2012;9:3. doi:10.1186/1743-8977-9-3.
30. Kawakami T, Ando T, Kimura M, Wilson BS, Kawakami Y. Mast cells in atopic dermatitis. Curr Opin Immunol. 2009;21(6):666–78. doi:10.1016/j.coi.2009.09.006.
31. Stone KD, Prussin C, Metcalfe DD. IgE, mast cells, basophils, and eosinophils. J Allergy Clin Immunol. 2010;125(2 Suppl 2):S73–80. doi:10.1016/j.jaci.2009.11.017.
32. Strait RT, Morris SC, Finkelman FD. IgG-blocking antibodies inhibit IgE-mediated anaphylaxis *in vivo* through both antigen interception and Fc gamma RIIb cross-linking. J Clin Invest. 2006;116(3):833–41. doi:10.1172/JCI25575.
33. Uermosi C, Beerli RR, Bauer M, Manolova V, Dietmeier K, Buser RB, et al. Mechanisms of allergen-specific desensitization. J Allergy Clin Immunol. 2010;126(2):375–83. doi:10.1016/j.jaci.2010.05.040.
34. Cassard L, Jonsson F, Arnaud S, Daeron M. Fcgamma receptors inhibit mouse and human basophil activation. J Immunol. 2012;189(6):2995–3006. doi:10.4049/jimmunol.1200968.
35. Jutel M, Jaeger L, Suck R, Meyer H, Fiebig H, Cromwell O. Allergen-specific immunotherapy with recombinant grass pollen allergens. J Allergy Clin Immunol. 2005;116(3):608–13. doi:10.1016/j.jaci.2005.06.004.
36. Akdis M, Akdis CA. Mechanisms of allergen-specific immunotherapy: multiple suppressor factors at work in immune tolerance to allergens. J Allergy Clin Immunol. 2014;133(3):621–31. doi:10.1016/j.jaci.2013.12.1088.
37. Nel AE, Madler L, Velegol D, Xia T, Hoek EM, Somasundaran P, et al. Understanding biophysicochemical interactions at the nano-bio interface. Nat Mater. 2009;8(7):543–57. doi:10.1038/nmat2442.
38. Jiang J, Oberdo¨rster Gn, Biswas P. Characterization of size, surface charge, and agglomeration state of nanoparticle dispersions for toxicological studies. J Nanoparticle Res. 2009;11(1):77–89.
39. Boverhof DR, David RM. Nanomaterial characterization: considerations and needs for hazard assessment and safety evaluation. Anal Bioanal Chem. 2010;396(3):953–61. doi:10.1007/s00216-009-3103-3.
40. Chapman MD, Platts-Mills TA. Measurement of IgG, IgA and IgE antibodies to Dermatophagoides pteronyssinus by antigen-binding assay, using a partially purified fraction of mite extract (F4P1). Clin Exp Immunol. 1978;34(1):126–36.
41. Platts-Mills TA. Local production of IgG, IgA and IgE antibodies in grass pollen hay fever. J Immunol. 1979;122(6):2218–25.
42. Soderstrom L, Lilja G, Borres MP, Nilsson C. An explorative study of low levels of allergen-specific IgE and clinical allergy symptoms during early childhood. Allergy. 2011;66(8):1058–64. doi:10.1111/j.1398-9995.2011.02578.x.
43. Morokata T, Ishikawa J, Yamada T. Antigen dose defines T helper 1 and T helper 2 responses in the lungs of C57BL/6 and BALB/c mice independently of splenic responses. Immunol Lett. 2000;72(2):119–26.
44. Riedl MA, Landaw EM, Saxon A, Diaz-Sanchez D. Initial high-dose nasal allergen exposure prevents allergic sensitization to a neoantigen. J Immunol. 2005;174(11):7440–5.
45. Baroli B. Penetration of nanoparticles and nanomaterials in the skin: fiction or reality? J Pharm Sci. 2010;99(1):21–50. doi:10.1002/jps.21817.
46. Platts-Mills TA, Vaughan JW, Blumenthal K, Pollart Squillace S, Sporik RB. Serum IgG and IgG4 antibodies to Fel d 1 among children exposed to 20 microg Fel d 1 at home: relevance of a nonallergic modified Th2 response. Int Arch Allergy Immunol. 2001;124(1–3):126–9.
47. Matsui EC, Diette GB, Krop EJ, Aalberse RC, Smith AL, Curtin-Brosnan J, et al. Mouse allergen-specific immunoglobulin G and immunoglobulin G4 and allergic symptoms in immunoglobulin E-sensitized laboratory animal workers. Clin Exp Allergy. 2005;35(10):1347–53. doi:10.1111/j.1365-2222.2005.02331.x.
48. Jeal H, Draper A, Harris J, Taylor AN, Cullinan P, Jones M. Modified Th2 responses at high-dose exposures to allergen: using an occupational model. Am J Respir Crit Care Med. 2006;174(1):21–5. doi:10.1164/rccm.200506-964OC.
49. Ilves M, Palomaki J, Vippola M, Lehto M, Savolainen K, Savinko T, et al. Topically applied ZnO nanoparticles suppress allergen induced skin inflammation but induce vigorous IgE production in the atopic dermatitis mouse model. Part Fibre Toxicol. 2014;11:38. doi:10.1186/s12989-014-0038-4.
50. Schilling K, Bradford B, Castelli D, Dufour E, Nash JF, Pape W, et al. Human safety review of "nano" titanium dioxide and zinc oxide. Photochem Photobiol Sci. 2010;9(4):495–509. doi:10.1039/b9pp00180h.

OBSTETRICS

Hydroxylated fullerene: a potential antiinflammatory and antioxidant agent for preventing mouse preterm birth

Tetsu Wakimoto, MD; Kaoru Uchida, PhD; Kazuya Mimura, MD; Takeshi Kanagawa, MD; Tzvetozar Roussev Mehandjiev, MD; Hisae Aoshima, PhD; Ken Kokubo, PhD; Nobuaki Mitsuda, MD, PhD; Yasuo Yoshioka, PhD; Yasuo Tsutsumi, PhD; Tadashi Kimura, MD, PhD; Itaru Yanagihara, MD, PhD

OBJECTIVE: Intrauterine infection such as by *Escherichia coli* and *Ureaplasma* spp induce placental inflammation and are one of the leading causes of preterm birth. Here we evaluated hydroxylated fullerene ($C_{60}[OH]_{44}$) for its in vitro antiinflammatory and antioxidant effects against host cellular responses to the ureaplasma toll-like receptor 2 (TLR2) ligand, UPM-1. In addition, we investigated the preventative effects of $C_{60}(OH)_{44}$ in vivo in a mouse preterm birth model that used UPM-1.

STUDY DESIGN: TLR2-overexpressing cell lines and the primary cultures of mouse peritoneal macrophages were pretreated with $C_{60}(OH)_{44}$. After UPM-1 addition to the cell lines, the activation of the nuclear factor kappa-light chain-enhancer of activated B cells (NF-kappaB) signaling cascade and the production of reactive oxygen species were monitored. The levels of expression of inflammatory cytokines of interleukin (IL)-6, IL-1β, tumor necrosis factor (TNF)-α, and the production of reactive oxygen species were quantified after stimulation with UPM-1. The in vivo preventative effects of $C_{60}(OH)_{44}$ on mice preterm birth were evaluated by analyzing the preterm birth rates and fetal survival rates in the preterm birth mouse model with placental histological analyses.

RESULTS: Pretreatment with $C_{60}(OH)_{44}$ significantly suppressed UPM-1-induced NF-kappaB activation and reactive oxygen species production in TLR2-overexpressing cell lines. In the primary culture of mouse peritoneal macrophages, UPM-1-induced production of reactive oxygen species and the expression of inflammatory cytokines such as IL-6, IL-1β, and TNF-α were significantly reduced by pretreatment with $C_{60}(OH)_{44}$. In the UPM-1-induced preterm birth mouse model, the preterm birth rate decreased from 72.7% to 18.2% after an injection of $C_{60}(OH)_{44}$. Placental examinations of the group injected with $C_{60}(OH)_{44}$ reduced the damage of the spongiotrophoblast layer and reduced infiltration of neutrophils.

CONCLUSION: $C_{60}(OH)_{44}$ was effective as a preventative agent of preterm birth in mice.

Key words: hydroxylated fullerene, nuclear factor-kappaB, preterm birth mouse, reactive oxygen species, ureaplasma membrane-1

Cite this article as: Wakimoto T, Uchida K, Mimura K, et al. Hydroxylated fullerene: a potential antiinflammatory and antioxidant agent for preventing mouse preterm birth. Am J Obstet Gynecol 2015;213:708.e1-9.

The World Health Organization has defined preterm birth as birth that occurs prior to the 37th gestational week.[1] The estimated number of preterm births worldwide was 15 million in 2010 (11.1%).[2] Preterm birth is a risk factor in more than 50% of all incidents of perinatal mortality and infantile respiratory failure, and it results in long-term neurologic morbidity.[2,3]

Babies born before 28 gestational weeks have a risk of disease during childhood and a risk of cerebrovascular and ischemic heart disease in early adulthood.[4] The development of perinatal care has raised the survival rate of infants with extremely low birthweights,[5] which resulted in the recent

From the Department of Obstetrics and Gynecology, Graduate School of Medicine (Drs Wakimoto, Mimura, Kanagawa, Mehandjiev, and Kimura), Division of Applied Chemistry, Graduate School of Engineering (Dr Kokubo), Department of Toxicology and Safety Science, Graduate School of Pharmaceutical Sciences (Dr Yoshioka and Tsutsumi), and Vaccine Creation Project, BIKEN Innovative Vaccine Research Alliance Laboratories, Research Institute for Microbial Diseases (Dr Yoshioka), Osaka University; Department of Developmental Medicine, Research Institute (Drs Wakimoto, Uchida, Mehandjiev, and Yanagihara), and Department of Maternal-Fetal Medicine (Dr Mitsuda), Osaka Medical Center for Maternal and Child Health; and Vitamin C60 BioResearch Corporation (Dr Aoshima), Osaka, Japan. Dr Uchida is currently with the Faculty of Food and Nutrition, Kyushu Welfare University, Fukuoka, Japan.

Received March 3, 2015; revised May 15, 2015; accepted July 13, 2015.

This study was supported in part by grants-in-aid from the Ministry of Education, Culture, Sports, Science, and Technology (26461652, 23591609) and by SENTAN, JST, Japan.

The authors report no conflict of interest.

Corresponding author: Itaru Yanagihara, MD, PhD. itaruy@mch.pref.osaka.jp

0002-9378/$36.00 • http://dx.doi.org/10.1016/j.ajog.2015.07.017

observation that females born preterm have an increased risk of reproductive difficulties.[6] Considerable efforts have been focused on the control of preterm birth; however, the preterm birth rate is still increasing.[7]

It is widely accepted that intrauterine bacterial infections are one of the most important causes of preterm birth.[8] Lipopolysaccharide (LPS) from *Escherichia coli*, which is a ligand of the toll-like receptor (TLR) 4, activates downstream inflammatory responses.[9,10] LPS has often been used in mammalian models of preterm birth.[11-13]

There is growing evidence that *Ureaplasma* spp, belonging to the family *Mycoplasmataceae*, has been a common causative bacteria of chorioamnionitis (CAM) and, consequently, preterm birth.[14-16] Patients with threatened preterm birth and intact membranes who test positive on polymerase chain reaction (PCR) for *U urealyticum* in the amniotic fluid are at risk of going into preterm birth with adverse perinatal outcomes.[17]

We analyzed 151 preterm and stillbirth placentas, and 63 (42%) of them were positive for *Ureaplasma* spp.[18] Although *Ureaplasma* spp has been considered to be involved in the pathobiology of preterm birth for more than half a century, the mechanism of its involvement remains unclear. Synthesized diacylated 21 N-terminal amino acids of the ureaplasmal outer membrane lipoprotein (UPM-1) activates the signaling cascade of nuclear factor-kappa—light-chain enhancer of activated B cells (NF-kappaB) through TLR2. UPM-1 has been shown to induce preterm birth and intrauterine fetal death in C3H/HeN mice.[19]

Fullerene, a nanomaterial with radical-scavenging activity, is a molecule that comprises carbon in the form of a hollow sphere.[20-24] These observations suggest fullerene is an antioxidant agent. In our previous study, we demonstrated injections of the 70 nm silica nanoparticle restricted fetal growth and induced abortion in pregnant mice. However, fullerene did not cause any pregnancy-associated complications at the dose used in our study.[25]

In this study, we aimed to clarify the antiinflammatory and antioxidant effects of water-soluble hydroxylated fullerene ($C_{60}[OH]_{44}$) on TLR2-mediated inflammation in vitro. We found that $C_{60}(OH)_{44}$ suppressed the inflammation and the production of reactive oxygen species in cultured cells. Furthermore, $C_{60}(OH)_{44}$ reduced preterm birth and fetal loss in our UPM-1—induced preterm mouse model, suggesting $C_{60}(OH)_{44}$ has potential as a therapeutic agent for preterm birth in mice.

Materials and Methods

Cell culture and $C_{60}(OH)_{44}$ cytotoxicity

Hydroxylated fullerene [$C_{60}(OH)_{44}$], which has an average molecular formula of $C_{60}(OH)_{44}\cdot 8H_2O$, was synthesized with hydrogen peroxide, according to a previously reported method.[26]

HeLa and HEK293T cells lines were purchased from RIKEN (Saitama, Japan). The cells were maintained in Dulbecco's modified Eagle's medium (Sigma-Aldrich Co LLC, St. Louis, MO) containing 10% fetal calf serum, 100 U/mL of penicillin G, and 100 mg/mL of streptomycin under the condition of 5% CO_2 in humid air at 37°C. Both cell lines (6.0×10^3) were cultured overnight and exposed to various concentrations of $C_{60}(OH)_{44}$ (5, 10, 25, or 50 μM).

Cell viability was assayed with a cell-counting kit-8 (Dojindo Laboratories, Kumamoto, Japan) at different time points (24, 48, or 72 hours). In brief, we added 10 μL of the cell-counting kit-8 reagent at different time points and incubated for 2 hours. The optical density at a wavelength of 450 nm (OD_{450}) as absorbance was calculated with a microplate reader (Bio-Rad model 3550; Bio-Rad Laboratories, Hercules, CA). Cell viability was calculated as follows: [{(OD_{450}) of sample − (OD_{450}) of blank}/{(OD_{450}) of control − (OD_{450}) of blank}] × 100(%).

NF-kappaB reporter assay

An NF-kappaB reporter assay was conducted as previously described.[19] In brief, after an overnight culture of HeLa cells or HEK293T cells (2.4×10^4), 0.3 μg of pNF-kappaB-luciferase (Agilent Technologies, Santa Clara, CA), 0.1 μg of pFLAG-TLR2 and 0.1 μg of pRL-tk (Promega Corp, Madison, WI) were cotransfected with the lipofection reagent, FuGENE 6 (Promega Corp). After 48 hours of transfection, we added 0—50 μM of $C_{60}(OH)_{44}$. One hour after adding the reagents, the transfected cells were stimulated with 27.2 nM of UPM-1. After a further 8 hour exposure to UPM-1, the activated cells were lysed and a luciferase assay was performed with a dual-luciferase reporter assay system (Promega Corp) and quantified with a Luminescence Reader BLR-301 (Hitachi Aloka Medical, Ltd, Tokyo, Japan).

Flow cytometry for the detection of reactive oxygen species production in HEK293T cells

After the overnight culture of HEK293T cells (2.4×10^4), the cells were transfected with 0.4 μg of pF-TLR2 with FuGENE 6 (Promega Corp). Forty-eight hours after transfection, 50 μM of $C_{60}(OH)_{44}$ was added to the cells. One hour after adding the fullerene, the cells were stimulated with 27.2 nM of UPM-1. Eight hours after stimulation, 5 μM of the cellROX green reagent (Life Technologies, Carlsbad, CA) was added to the culture medium, and the relative fluorescence units (RFUs) of every 10,000 cells were measured with BD FACScalibur HG (Becton, Dickinson and Co, Franklin Lakes, NJ). The mean fluorescence was calculated with CellQuest Pro software (Becton, Dickson and Co).

Reactive oxygen species production of mouse peritoneal macrophages

C57BL/6J mice were from Japan SLC, Inc (Hamamatsu, Japan). The experimental protocols of the animal studies were approved by the animal experiment committee of Osaka Medical Center and the Research Institute for Maternal and Child Health.

Peritoneal macrophages were collected according to the method of Zhang et al[27] with a slight modification. In brief, 1—3 mL of 3% sterilized fluid thioglycollate medium II (Eiken Chemical Co, Ltd, Tokyo, Japan) was injected into the intraperitoneal cavities of 8—13 week old nonpregnant female mice.

Four days later, the refluxed intraperitoneal fluid was collected, and macrophages were kept in the RPMI 1640 medium (Sigma-Aldrich Co) containing 10% fetal calf serum, 100 U/mL of penicillin G, and 100 mg/mL of streptomycin. The next day, 1 hour prior to the stimulation of UPM-1 and LPS (*E coli* O55:B5; Sigma-Aldrich Co), we replaced the RPMI 1640 medium with a medium containing 50 μmol/L of $C_{60}(OH)_{44}$, and 8 hours after stimulation with 36.0 nM of UPM-1[19] and 1 μg/mL of LPS, we added 5 μmol/L of the CellROX green reagent (Life Technologies).

Reactive oxygen species (ROS) production was expressed in RFUs by using a fluorescence microscope (ECLIPSE TE-2000E; Nikon Corp, Tokyo, Japan) that was equipped with EM-CCD iXon+ (Andor Technology, Ltd, Belfast, UK), and the data were analyzed using Andor iQ2 software (Andor Technology, Ltd). At least 450 macrophages were quantified in each group.

Reverse transcription–polymerase chain reaction

We performed quantitative real-time polymerase chain reaction (qRT-PCR) to evaluate the inflammatory cytokines. Mouse peritoneal macrophages (1.95×10^6) were collected and stimulated as in the ROS production assay. After 8 hours of UPM-1 stimulation, total ribonucleic acid (RNA) was extracted with an SV RNA isolation kit (Promega Corp). First-strand complementary deoxyribonucleic acid was synthesized from 100 to 200 ng of RNA with random primers with a PrimeScript first-strand complementary deoxyribonucleic acid synthesis kit (Takara Bio Inc, Otsu, Japan).

qRT-PCR was performed to determine the levels of mouse interleukin (IL)-6, IL-1β, and tumor necrosis factor (TNF)-α with a QuantiTect SYBR Green PCR kit (QIAGEN Benelux B.V., Venlo, The Netherlands) on a Chromo 4 real-time PCR system (Bio-Rad Laboratories, Inc). The primers are listed in Table 1.[28,29] qRT-PCR was performed as follows: 40 cycles of 95°C for 20 seconds, 57°C for 30 seconds, and 72°C for 30 seconds.

TABLE 1
Set of primers used for PCR

Gene	Sequence	Product size, bp
Mouse IL-6	5'-tccagttgccttcttgggac-3'	331
	5'-gtactccagaagaccagagg-3'	
Mouse IL-1β	5'-ctccatgagctttgtacaagg-3'	245
	5'-tgctgatgtaccagttgggg-3'	
Mouse TNF-α	5'-gcatgatccgcgacgtggaa-3'	304
	5'-agatccatgccgttggccag-3'	

IL, interleukin; *PCR*, polymerase chain reaction; *TNF*, tumor necrosis factor.

Wakimoto. Hydroxylated fullerene for preventing mouse preterm birth. Am J Obstet Gynecol 2015.

Preterm birth mouse model

We used our previously reported preterm birth mouse model.[19] In brief, C3H/HeN mice (Japan SLC, Inc) were pair mated. We designated the day the vaginal plug was confirmed as day 0 of gestation. On day 14, a minilaparotomy was performed under isoflurane anesthesia. The uterus was exposed by incision to visualize all of the gestational sacs. The number of sacs was counted. Twenty microliters of UPM-1 (750 ng/μL, 0.27 mM; 5.4 nmol/body) or distilled water in the control group was injected into the uterus between the 2 lower gestational sacs on the right side of the uterus. Four hours after UPM-1 stimulation, 100 μg (68 nmol) of $C_{60}(OH)_{44}$ in 100 μL of phosphate-buffered saline (pH 7.4) was injected into the tail vein.

Forty-eight hours after exposure of the uterus to UPM-1, a cesarean delivery was performed, and the gestational sacs were checked. Preterm birth was detected when we could see at least 1 baby in the cage within 48 hours of the injection of UPM-1 or when we could not detect 1 gestational sac in the uterus when the cesarean delivery was performed. The number of live or dead pups in the uterus was recorded. Intrauterine fetal death was detected if white discoloration, markedly smaller fetal size, or maceration changes were observed.

Histological evaluations

The collected placentas were embedded in paraffin and stained with hematoxylin and eosin and a myeloid cell–specific esterase/naphthol AS-D chloroacetate esterase (3-hydroxy-2-naphthoic-o-toluidide chloroacetate) staining kit (Muto Pure Chemicals Co, Ltd, Tokyo, Japan). A light microscope (Olympus BX51; Olympus Corp, Tokyo, Japan) was used. The ratio of the spongiotrophoblast layer area to the total placental area was calculated according to previous reports.[5,19] In brief, the spongiotrophoblast layer and total placental areas were assessed with hematoxylin and eosin–stained sections and quantitatively analyzed with NIS-Elements Documentation, version 3.13 (Nikon Corp).[19]

Statistical analysis

PASW statistics 18 (IBM Corp, Armonk, NY) was used for the statistical analyses. Differences were considered statistically significant when $P < .05$. The data are expressed as mean ± SE for the cell viability analysis, NF-kappaB reporter assay.

To determine the dose dependency of $C_{60}(OH)_{44}$ against NF-kappaB activation, we conducted Pearson's regression analysis of the NF-kappaB reporter assay. For the quantification of ROS production, the mean fold of RFUs of the group of interest per RFU of the control group were calculated from 3 independent experiments of the flow cytometry analyses of every 10,000 cells or fluorescence microscopic observations of at least 450 cells.

Tukey's post hoc tests were performed with 1-way analyses of variance (ANOVAs) on the data from the previously mentioned experiments. For qRT-PCR of inflammatory cytokines of mouse peritoneal

FIGURE 1

The effect of $C_{60}(OH)_{44}$ in cell viability and NF-kappaB activation

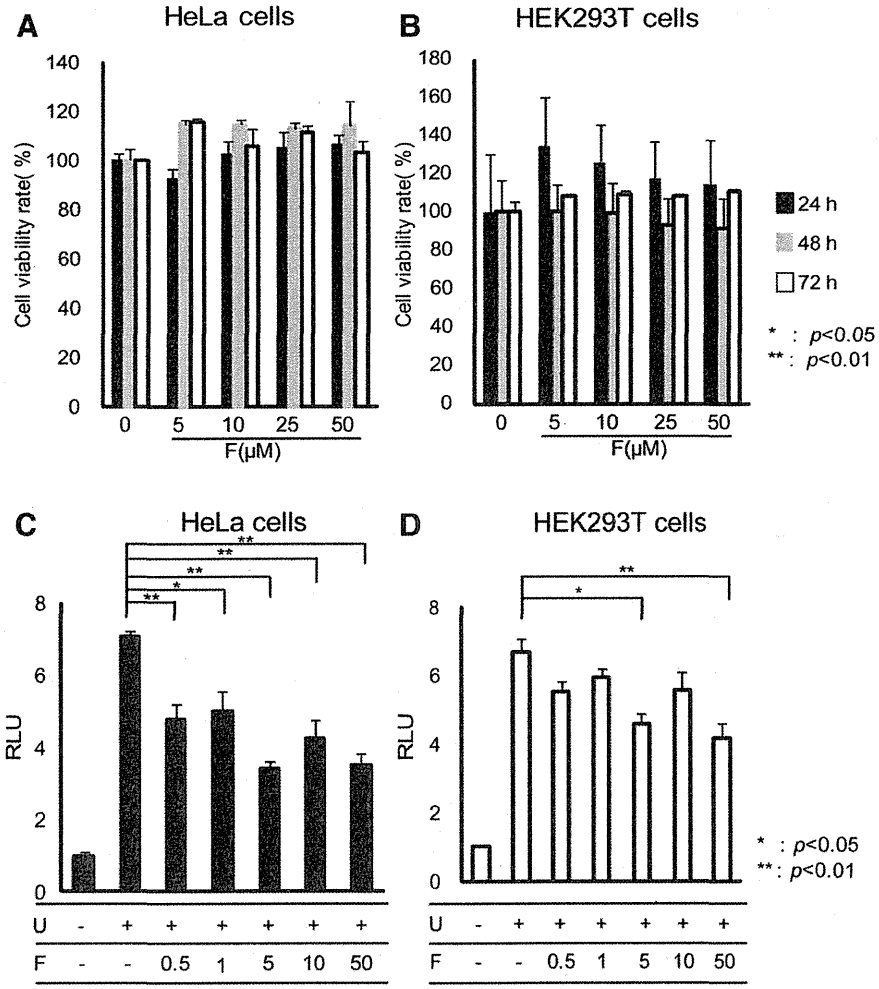

A, HeLa cells and **B,** HEK 293T cells were treated with various concentration of $C_{60}(OH)_{44}$ for 24 hours (mean ± SE, n = 4), 48 hours (n = 4), and 72 hours (n = 3). **C,** NF-kappaB activation was monitored in HeLa cells and **D,** HEK 293T cells with $C_{60}(OH)_{44}$ pretreatment prior to 27.2 nM UPM-1 stimulation (mean ± SE, n = 3). Statistical significant was determined by an ANOVA and the Tukey-Kramer post hoc test. *Asterisk* indicates $P < .05$, and *double asterisk* indicates $P < .01$.

ANOVA, analysis of variance; *$C_{60}(OH)_{44}$*, fullerene; *F*, hydroxylated $C_{60}(OH)_{44}$; *NF-kappaB*, nuclear factor-kappaB; *U*, 27.2 nM of UPM-1, ureaplasmal outer membrane.

Wakimoto. Hydroxylated fullerene for preventing mouse preterm birth. Am J Obstet Gynecol 2015.

macrophages, a nonparametric statistical analysis with the Kruskal-Wallis method was conducted from 3 independent experiments.

Fisher exact tests were applied to the data for the preterm birth. The fetal survival rate per dam was compared with 1-way ANOVAs with the Tukey-Kramer post hoc test.

In the histological examination, the ratios of the spongiotrophoblast layer to the placenta were analyzed by 1-way ANOVAs with Tukey's post hoc tests (6 placentas per group).

RESULTS

$C_{60}(OH)_{44}$ pretreatment inhibited activation of the NF-kappaB signal cascade

$C_{60}(OH)_{44}$ (0–50 μM) was added to the culture media of both cell lines. There was no significant difference in cell viability in both cell lines (Figure 1, A and B), which suggested the treatment with $C_{60}(OH)_{44}$ did not result in cellular toxicity at any of the concentrations or time points tested.

To investigate the inhibitory effects of $C_{60}(OH)_{44}$ pretreatment on inflammatory responses, we monitored NF-kappaB activation by using luciferase as a reporter in both cell lines. UPM-1–activated NF-kappaB signals were diminished by pretreatment with 50 μM of $C_{60}(OH)_{44}$ to 49.4% in HeLa cells ($P < .01$; Figure 1, C) and 75.0% in HEK293T cells ($P < .01$; Figure 1, D).

We conducted a Pearson's regression analysis to determine whether $C_{60}(OH)_{44}$ regulates NF-kappaB activation in a dose-dependent manner. In HeLa cells, it had a weak negative correlation in a dose-dependent manner ($r = -0.442$; $P = .066$). In HEK293T cells, it had a relatively strong negative correlation ($r = -0.617$; $P < .01$).

In vitro antioxidant activity and proinflammatory cytokine messenger RNA levels were suppressed by pretreatment with $C_{60}(OH)_{44}$

In HEK293T cells (Figure 2, A), UPM-1 activated ROS production by 1.83-fold, whereas 50 μM of $C_{60}(OH)_{44}$ suppressed it to background levels ($P < .01$).

We examined the influence of $C_{60}(OH)_{44}$ on ROS production in a primary culture of mouse peritoneal macrophages. Because the collected mouse macrophages adhered tightly to the culture plate dishes and the harvested cell count was relatively limited, we used a fluorescence microscopic analysis instead of a flow cytometric analysis. As shown in Figure 2, B, the fluorescence of ROS in each mouse macrophage was visualized as a green dot. The mean RFUs were measured. As in the HEK293T cells stimulated with UPM-1, UPM-1 increased the activation of ROS production by 1.58-fold in mouse macrophages. Pretreatment with 50 μM of $C_{60}(OH)_{44}$ significantly blocked the UPM-1–induced ROS production, which was at background levels ($P < .01$; Figure 2, B and C).

LPS (1.0 μg/mL), a TLR4 ligand, also increased ROS production by 1.99-fold compared with the control, whereas

pretreatment with 50 μmol/L of $C_{60}(OH)_{44}$ significantly blocked LPS-induced ROS production to the background level ($P < .01$; Figure 2, D and E).

We quantified the expression levels of the proinflammatory cytokine messenger RNA (mRNA) after stimulation with UPM-1 (Figure 3). Fifty micromoles of $C_{60}(OH)_{44}$ significantly inhibited IL-6 by 75% ($P = .027$), IL-1β by 72% ($P = .050$), and TNF-α by 84.1% ($P = .039$).

$C_{60}(OH)_{44}$ reduced mouse preterm deliveries in vivo

We evaluated whether $C_{60}(OH)_{44}$ had therapeutic effects in a mouse model of preterm birth. Preterm delivery was observed in 72.7% (8 of 11 dams) of the UPM-1–stimulated pregnant C3H/H3N mice, and these results corresponded with the 80% of the preterm deliveries found in our previous study.[19] The administration of $C_{60}(OH)_{44}$ significantly decreased the preterm birth rate to 18.2% (2 of 11 dams; $P < .05$) (Table 2). The fetal survival rate per dam after UPM-1 stimulation at 48 hours improved from 12.5% to 41.8% ($P = .086$) on treatment with $C_{60}(OH)_{44}$.

The ratio of the spongiotrophoblast layer area to the total placental area in the control group was 0.172, whereas in the UPM-1–administered group, it was 0.110. When $C_{60}(OH)_{44}$ was administered, the ratio improved to 0.147 (Figure 4, A). The intervillous space of the labyrinth layer of UPM-1–injected

FIGURE 2

The effect of $C_{60}(OH)_{44}$ against the ROS production

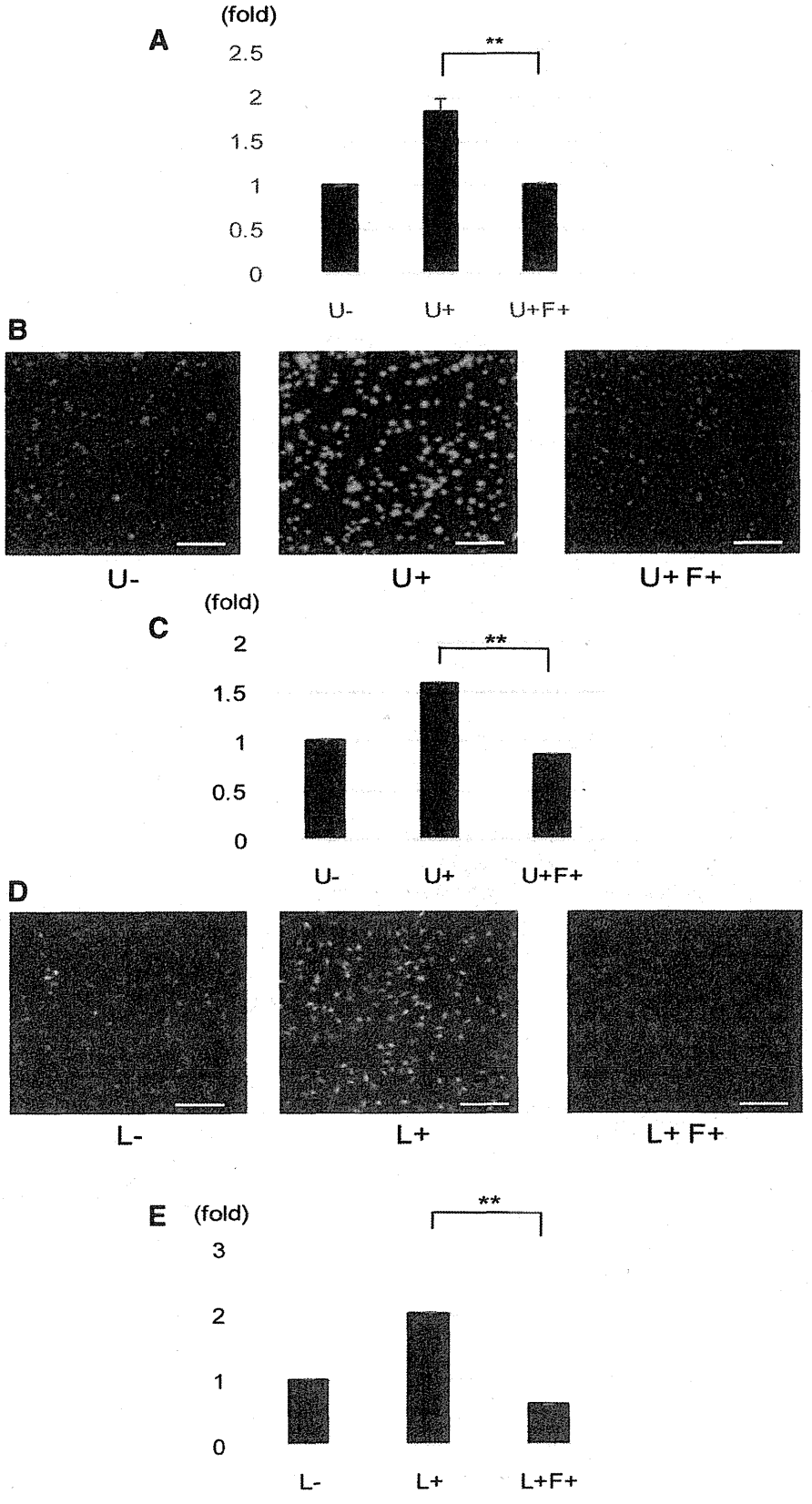

A, The inhibitory effect on the ROS production by pretreatment of 50 μM $C_{60}(OH)_{44}$ in HEK293T cells stimulated with 27.2 nM of UPM-1, in mouse peritoneal macrophages stimulated with **B** and **C**, 36.0 nM of UPM-1 (**B** and **C**), and with **D** and **E**, 1 μg/mL of LPS. For fold: RFU of the group of interest per RFU of control group (mean ± SE, n = 3). Scale bar is 100 μm. Statistical significant was determined by an ANOVA and the Tukey post hoc test. *Double asterisk* indicates $P < .01$.

ANOVA, analysis of variance; *$C_{60}(OH)_{44}$*, fullerene; *F*, hydroxylated $C_{60}(OH)_{44}$; *L*, lipopolysaccharide; *U*, UPM-1, ureaplasmal outer membrane 1.

Wakimoto. Hydroxylated fullerene for preventing mouse preterm birth. Am J Obstet Gynecol 2015.

FIGURE 3

The inhibitory effect of $C_{60}(OH)_{44}$ on inflammatory cytokine mRNA expression

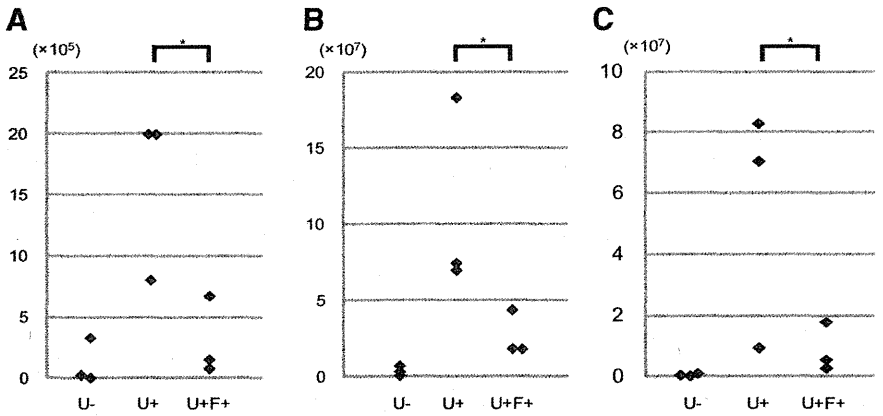

A, The mRNA expression of IL-6, **B,** IL-1β, and **C,** TNF-α were quantified (copies per 1 μg total RNA) by pretreatment of 50 μM $C_{60}(OH)_{44}$ in mouse peritoneal macrophage with 36.0 nM UPM-1 stimulation. Results are expressed as scatter plots (n = 3). Statistical significance was determined with the Kruskal-Wallis method. *Asterisk* indicates $P < .05$.

$C_{60}(OH)_{44}$, fullerene; *F*, hydroxylated $C_{60}(OH)_{44}$; *mRNA*, messenger ribonucleic acid; *TNF*, tumor necrosis factor; *U*, UPM-1, ureaplasmal outer membrane 1.

Wakimoto. Hydroxylated fullerene for preventing mouse preterm birth. Am J Obstet Gynecol 2015.

mice increased, accompanied by a loss of circulated blood cells compared with that of controls (Figure 4, E and F), which was consistent with the findings of our previous report.[19]

In the $C_{60}(OH)_{44}$-treated placentas, the intervillous space was narrower and filled with blood cells, which suggested that the vascular tonus of the labyrinth layer could recuperate with the appropriate blood supply (Figure 4, G). Neutrophil infiltration in the preterm placenta is one of the hallmarks of human histological CAM. UPM-1 induced neutrophil infiltration, especially on the edge of the placenta (Figure 4, H and I). In contrast, neutrophil infiltration in the placenta diminished after $C_{60}(OH)_{44}$ injections (Figure 4, J).

Comment

Preterm birth is frequently caused by intrauterine infection, associated with CAM[18] and fetal inflammatory response syndrome.[30] Recent advances in immunology have clarified the major molecular mechanisms underlying the interactions between the host and bacteria are bridged by TLR and TLR ligands.[31]

Fullerene and its derivatives have powerful antioxidant effects. A fullerene molecule can absorb at least 34 radicals.[20] A fullerene molecule has the lowest unoccupied molecular orbital, which allows it to easily react with radical species and take up 1 electron from them, making them nontoxic.[32]

Several reports have indicated a direct connection between TLR signaling and ROS synthesis. TLR (TLR1, TLR2, and TLR4) signals enhance ROS production, which is achieved by the translocation of the TNF receptor-associated factor 6 into mitochondria, which induces the ubiquitination of the evolutionarily conserved signaling intermediate in the Toll pathway.[33] ROS forms a disulfide bond between Cys54 and Cys347 in the IKKγ/Nemo protein complex, resulting in the phosphorylation of the NF-kappaB inhibitor-α and activation of NF-kappaB.[34]

From these observations, we hypothesized regulating excess ROS production with $C_{60}(OH)_{44}$ may negatively control UPM-1–induced TLR2 signal cascades. We monitored the inhibitory effects of $C_{60}(OH)_{44}$ on NF-kappaB activity, ROS, and inflammatory cytokines induced by the TLR2 ligand UPM-1.

TLR2 and TLR4 were up-regulated in the uterus and cervix in pregnant mice[35] and in the ectocervical epithelium in pregnant women.[36] TLR2 and TLR4 were also up-regulated in the uterus, cervix, and placenta in an LPS-induced infectious preterm birth mouse model.[37] TLR2 expression was increased in the human spontaneous preterm birth membrane with histological CAM, regardless of intact or ruptured membranes.[38] These observations may advocate the idea that the immune cells were activated during intrauterine infection.

Fullerenes are generally hydrophobic molecules that are extremely small in size. Hydrophilic addends, such as the hydroxyl group, leads to the formation of various polyhydroxylated fullerenes, including $C_{60}(OH)_n$. The enhancement

TABLE 2

Pregnancy outcome in mice administered with UPM-1 and hydroxylated fullerene ($C_{60}[OH]_{44}$)

Dams	Preterm birth (preterm birth rate, %)	Fetal survival rate per dam, %
Control (n = 5)	0/5 (0)	85.8
UPM-1 (n = 11)	8/11 (72.7)	12.5
F (n = 6)	0/6 (0%)	78.9
UPM-1 plus F (n = 11)	2/11 (18.2)[a]	41.8

Statistical significance was determined by a Fisher exact test.

F, hydroxylated fullerene [$C_{60}(OH)_{44}$] (100 μg/dam); *UPM-1*, synthesized TLR2 agonist, diacylated lipoprotein, derived from ureaplasmal outer membrane.

[a] $P < .05$.

Wakimoto. Hydroxylated fullerene for preventing mouse preterm birth. Am J Obstet Gynecol 2015.

FIGURE 4

The effect of $C_{60}(OH)_{44}$ treatment in preterm birth mouse model placenta

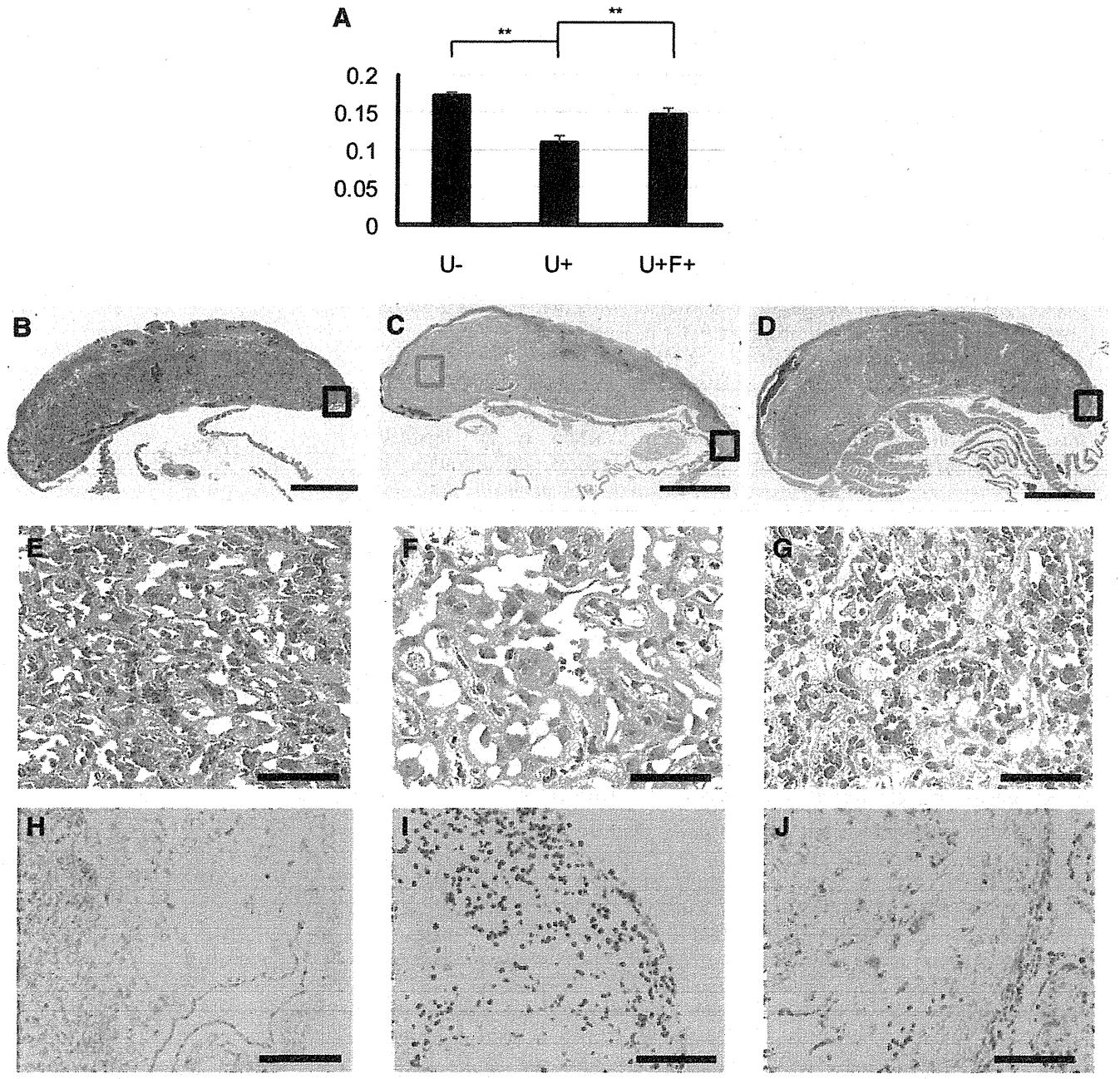

A, Spongiotrophoblast layer area per total placental area ratio of 6 placentas in each group were shown in panel. **B-G**, Hematoxylin and eosin stains. **B, E,** and **H**, Negative control placenta. **C, F,** and **I**, UPM-1—administered mice placenta. **D, G,** and **J**, UPM-1 plus $C_{60}(OH)_{44}$—administered mice placenta. Scale bar is 1 mm (**B, C,** and **D**). The magnified figures in the *blue box—shaped area*. Scale bar is 10 μm (**E, F,** and **G**). The magnified figures in the *black box—shaped area* with (3-hydroxy-2-naphthoic-o-toluidide chloroacetate) neutrophil esterase AS-D stain. Scale bar is 100 μm (**H, I,** and **J**). Statistical significance was determined by an ANOVA and a Tukey-Kramer post hoc test. *Double asterisk* indicates $P < .01$.

ANOVA, analysis of variance; *$C_{60}(OH)_{44}$*, fullerene; *F*, hydroxylated $C_{60}(OH)_{44}$; *U*, UPM-1, ureaplasmal outer membrane 1.

Wakimoto. Hydroxylated fullerene for preventing mouse preterm birth. Am J Obstet Gynecol 2015.

of hydrophilicity correlated with the increased number of hydroxyl groups in fullerenes.

$C_{60}(OH)_{24}$ displayed toxicity to the rat hepatocyte at a concentration of 50 μmol/L[39] and decreased mitochondrial membrane potential ($\Delta\psi$) at a concentration of 125 μmol/L.[40] $C_{60}(OH)_{6\text{-}12}$ (~30 μmol/L) showed toxicity against

human hepatoma HepG2 cells and rat hepatoma dRLh-84 cells, whereas C_{60}, $C_{60}(OH)_2$, and $C_{60}(OH)_{36}$ did not reveal any cytotoxicity at the same concentration.[41]

In our experiments, we used relatively hydrophilic [$C_{60}(OH)_{44}$], which did not induce any cell toxicity in the HeLa cells or HEK293T cells at a concentration of 50 μmol/L (Figure 1, A and B). These observations indicate that local hydrophobicity may be a mediator of the cytotoxicity of fullerenes.

To test the reproductive toxicity of $C_{60}(OH)_{44}$ in the pregnant mouse, we administered a 5 times higher dose (500 μg [340 nmol]) via a tail-vein injection. This high dose of $C_{60}(OH)_{44}$ did not cause maternal death (0 of 5 dams), preterm birth (0 of 5 dams), or decrease fetal survival rate per dam (89.8%).

There are a few reports describing the immunostimulatory effects of fullerenes. Liu et al[42] reported $C_{60}(OH)_{20}$ fullerene increased TNF-α in murine T lymphocytes and macrophages. The opposite immunomodulatory actions of fullerene may be due to the concentration of fullerene or its hydrophobicity. We used $C_{60}(OH)_{44}$ at a concentration of 50 μM, whereas Liu et al used 100 μM of $C_{60}(OH)_{20}$. The higher concentration of less hydrophilic fullerene may result in the molecular aggregation in vitro, which prevents the immunosuppressive activity of fullerene.[26]

A guarantee of safety of an agent is one of the most important issues that need to be determined before in vivo clinical use, and many reports have shown fullerene derivatives rarely exhibit toxicity in vivo and in vitro.[21,42-44] In addition, we reported polyvinylpyrrolidone (PVP)-fullerene did not exhibit reproductive toxicity when we injected intravenously in pregnant mice.[25]

In addition, Baati et al[44] orally administered pristine fullerene dissolved in olive oil orally to rats, and the rats did not show any chronic toxicity and surprisingly doubled their life span. In accordance with these previous reports, our data also showed $C_{60}(OH)_{44}$ did not have any cell toxicity (Figure 1, A and B). Furthermore, $C_{60}(OH)_{44}$ alone did not cause intrauterine fetal death, even when administered at 5 times higher doses (Table 2).

In the placental histological examinations (Figure 4), UPM-1 caused dilatation of the intervillous space of the labyrinth layer and destroyed the spongiotrophoblast layer. $C_{60}(OH)_{44}$ reduced these morphological changes. Neutrophil infiltration was significantly reduced by $C_{60}(OH)_{44}$. The intravenous administration of $C_{60}(OH)_{44}$ ameliorated the intrauterine inflammatory environment and had a trend to increase the pup survival rate from that resulting from the UPM-1 injection.

In this report, we selected the intravenous injections of $C_{60}(OH)_{44}$ in accordance with our previous report.[25] However, Tsuchiya et al[45] reported the intraperitoneal administration of PVP-fullerene to pregnant mice on gestational day 11 resulted in fetal head, tail abnormalities, or fetal death. However in that study, the authors administered 25–137 mg/kg of PVP-fullerene, whereas we administered 0.1–0.5 mg/dam (3.3–5 mg/kg). Further study is needed to determine the optimal dose and administration route.

There is a report of the cross-placental transfer of ~0.3 mg/kg ^{14}C-labeled C_{60} injected into pregnant rats on gestational day 15.[46] Thereafter, 2% of ^{14}C-labeled C_{60} was detected in the placenta, 0.87% in the fetus, and 0.036% in the fetal brain. Moreover, the report showed that ^{14}C-labeled C_{60} was secreted into milk and lactating dams had the particle.

The genotoxicity of this molecule was tested on male and female mice, and C_{60} (20–78 mg/kg) did not cause in vivo cytogenetic damage in the bone marrow cells of the male and female mice.[47] Intravenous administration of 10 mg/kg of $C_{60}(OH)_{30}$ did not show any changes on the analysis of blood in female rats.[48]

There are no published reports of radiolabeled or fluorescence-labeled fullerene [$C_{60}(OH)_{44}$]; therefore, pharmacokinetics of $C_{60}(OH)_{44}$ have not yet been clarified. This is a scientific limitation of our experiments, and further study will be needed to elucidate these aspects.

In conclusion, this is the first report hydroxylated fullerene [$C_{60}(OH)_{44}$] prevented TLR ligand–induced preterm birth in mice. These findings suggest $C_{60}(OH)_{44}$ is a promising agent for the prevention of preterm birth. ■

ACKNOWLEDGMENT

We thank Dr F. Nishiumi, MCHRI, for helpful discussions.

REFERENCES

1. World Health Organization recommended definitions, terminology and format for statistical tables related to the perinatal period and use of a new certificate for cause of perinatal deaths. Modifications recommended by FIGO as amended October 14, 1976. Acta Obstet Gynecol Scand 1977;56:247-53.

2. Blencowe H, Cousens S, Chou D, et al. Born too soon: the global epidemiology of 15 million preterm births. Reprod Health 2013;10(Suppl 1):S2.

3. Goldenberg RL, Hauth JC, Andrews WW. Intrauterine infection and preterm delivery. N Engl J Med 2000;342:1500-7.

4. Ueda P, Cnattingius S, Stephansson O, Ingelsson E, Ludvigsson JF, Bonamy AK. Cerebrovascular and ischemic heart disease in young adults born preterm: a population-based Swedish cohort study. Eur J Epidemiol 2014;29:253-60.

5. Eichenwald EC, Stark AR. Management and outcomes of very low birth weight. N Engl J Med 2008;358:1700-11.

6. Swamy GK, Ostbye T, Skjaerven R. Association of preterm birth with long-term survival, reproduction, and next-generation preterm birth. JAMA 2008;299:1429-36.

7. Blencowe H, Cousens S, Oestergaard MZ, et al. National, regional, and worldwide estimates of preterm birth rates in the year 2010 with time trends since 1990 for selected countries: a systematic analysis and implications. Lancet 2012;379:2162-72.

8. Carey JC, Klebanoff MA. Is a change in the vaginal flora associated with an increased risk of preterm birth? Am J Obstet Gynecol 2005;192:1341-6.

9. Lien E, Means TK, Heine H, et al. Toll-like receptor 4 imparts ligand-specific recognition of bacterial lipopolysaccharide. J Clin Invest 2000;105:497-504.

10. Poltorak A, He X, Smirnova I, et al. Defective LPS signaling in C3H/HeJ and C57BL/10ScCr mice: mutations in Tlr4 gene. Science (New York, NY) 1998;282:2085-8.

11. Elovitz MA, Wang Z, Chien EK, Rychlik DF, Phillippe M. A new model for inflammation-induced preterm birth: the role of platelet-activating factor and Toll-like receptor-4. Am J Pathol 2003;163:2103-11.

12. Agrawal V, Smart K, Jilling T, Hirsch E. Surfactant protein (SP)-A suppresses preterm

delivery and inflammation via TLR2. PloS One 2013;8:e63990.
13. Celik H, Ayar A. Effects of erythromycin on pregnancy duration and birth weight in lipopolysaccharide-induced preterm labor in pregnant rats. Eur J Obstet Gynecol Reprod Biol 2002;103:22-5.
14. Viscardi RM. Ureaplasma species: role in diseases of prematurity. Clin Perinatol 2010;37: 393-409.
15. Capoccia R, Greub G, Baud D. Ureaplasma urealyticum, Mycoplasma hominis and adverse pregnancy outcomes. Curr Opin Infect Dis 2013;26:231-40.
16. Larsen B, Hwang J. Mycoplasma, Ureaplasma, and adverse pregnancy outcomes: a fresh look. Infect Dis Obstet Gynecol 2010;521921:12.
17. Yoon BH, Romero R, Lim J-H, et al. The clinical significance of detecting Ureaplasma urealyticum by the polymerase chain reaction in the amniotic fluid of patients with preterm labor. Am J Obstet Gynecol 2003;189:919-24.
18. Namba F, Hasegawa T, Nakayama M, et al. Placental features of chorioamnionitis colonized with Ureaplasma species in preterm delivery. Pediatr Res 2010;67:166-72.
19. Uchida K, Nakahira K, Mimura K, et al. Effects of Ureaplasma parvum lipoprotein multiple-banded antigen on pregnancy outcome in mice. J Reprod Immunol 2013;100:118-27.
20. Krusic PJ, Wasserman E, Keizer PN, Morton JR, Preston KF. Radical reactions of c60. Science (New York, NY) 1991;254:1183-5.
21. Gharbi N, Pressac M, Hadchouel M, Szwarc H, Wilson SR, Moussa F. [60]Fullerene is a powerful antioxidant in vivo with no acute or subacute toxicity. Nano Lett 2005;5: 2578-85.
22. Yin JJ, Lao F, Fu PP, et al. The scavenging of reactive oxygen species and the potential for cell protection by functionalized fullerene materials. Biomaterials 2009;30:611-21.
23. Huang ST, Ho CS, Lin CM, Fang HW, Peng YX. Development and biological evaluation of C(60) fulleropyrrolidine-thalidomide dyad as a new anti-inflammation agent. Bioorg Med Chem 2008;16:8619-26.
24. Theriot CA, Casey RC, Moore VC, et al. Dendro[C(60)]fullerene DF-1 provides radioprotection to radiosensitive mammalian cells. Radiat Environ Biophys 2010;49:437-45.
25. Yamashita K, Yoshioka Y, Higashisaka K, et al. Silica and titanium dioxide nanoparticles cause pregnancy complications in mice. Nat Nanotechnol 2011;6:321-8.
26. Kokubo K, Shirakawa S, Kobayashi N, Aoshima H, Oshima T. Facile and scalable synthesis of a highly hydroxylated water-soluble fullerenol as a single nanoparticle. Nano Res 2011;4:204-15.
27. Zhang X, Goncalves R, Mosser DM. The isolation and characterization of murine macrophages. Curr Protoc Immunol 2008. Chapter 14:Unit 14.1.
28. Kawane K, Tanaka H, Kitahara Y, Shimaoka S, Nagata S. Cytokine-dependent but acquired immunity-independent arthritis caused by DNA escaped from degradation. Proc Natl Acad Sci USA 2010;107:19432-7.
29. Ramesh G, Zhang B, Uematsu S, Akira S, Reeves WB. Endotoxin and cisplatin synergistically induce renal dysfunction and cytokine production in mice. Am J Physiol Renal Physiol 2007;293:F325-32.
30. Gotsch F, Romero R, Kusanovic JP, et al. The fetal inflammatory response syndrome. Clin Obstet Gynecol 2007;50:652-83.
31. Takeda K, Akira S. TLR signaling pathways. Semin Immunol 2004;16:3-9.
32. Bakry R, Vallant RM, Najam-ul-Haq M, et al. Medicinal applications of fullerenes. Int J Nanomed 2007;2:639-49.
33. West AP, Brodsky IE, Rahner C, et al. TLR signalling augments macrophage bactericidal activity through mitochondrial ROS. Nature 2011;472:476-80.
34. Herscovitch M, Comb W, Ennis T, et al. Intermolecular disulfide bond formation in the NEMO dimer requires Cys54 and Cys347. Biochem Biophys Res Commun 2008;367:103-8.
35. Gonzalez JM, Xu H, Ofori E, Elovitz MA. Toll-like receptors in the uterus, cervix, and placenta: is pregnancy an immunosuppressed state? Am J Obstet Gynecol 2007;197:296.e1-6.
36. Lashkari BS, Shahana S, Anumba DO. Toll-like receptor 2 and 4 expression in the pregnant and non-pregnant human uterine cervix. J Reprod Immunol 2015;107:43-51.
37. Elovitz MA, Mrinalini C. Can medroxyprogesterone acetate alter Toll-like receptor expression in a mouse model of intrauterine inflammation? Am J Obstet Gynecol 2005;193: 1149-55.
38. Kim YM, Romero R, Chaiworapongsa T, et al. Toll-like receptor-2 and -4 in the chorioamniotic membranes in spontaneous labor at term and in preterm parturition that are associated with chorioamnionitis. Am J Obstet Gynecol 2004;191:1346-55.
39. Nakagawa Y, Inomata A, Ogata A, Nakae D. Comparative effects of sulfhydryl compounds on target organellae, nuclei and mitochondria, of hydroxylated fullerene-induced cytotoxicity in isolated rat hepatocytes. J Appl Toxicol 2015;23.
40. Nakagawa Y, Suzuki T, Ishii H, Nakae D, Ogata A. Cytotoxic effects of hydroxylated fullerenes on isolated rat hepatocytes via mitochondrial dysfunction. Arch Toxicol 2011;85: 1429-40.
41. Shimizu K, Kubota R, Kobayashi N, et al. Cytotoxic effects of hydroxylated fullerenes in three types of liver cells. Materials 2013;6: 2713-22.
42. Liu Y, Jiao F, Qiu Y, et al. Immunostimulatory properties and enhanced TNF- alpha mediated cellular immunity for tumor therapy by C60(OH) 20 nanoparticles. Nanotechnology 2009;20: 415102.
43. Takahashi M, Kato H, Doi Y, et al. Sub-acute oral toxicity study with fullerene C60 in rats. J Toxicol Sci 2012;37:353-61.
44. Baati T, Bourasset F, Gharbi N, et al. The prolongation of the lifespan of rats by repeated oral administration of [60]fullerene. Biomaterials 2012;33:4936-46.
45. Tsuchiya T, Oguri I, Yamakoshi YN, Miyata N. Novel harmful effects of [60]fullerene on mouse embryos in vitro and in vivo. FEBS Lett 1996;393:139-45.
46. Sumner SC, Fennell TR, Snyder RW, Taylor GF, Lewin AH. Distribution of carbon-14 labeled C60 ([14C]C60) in the pregnant and in the lactating dam and the effect of C60 exposure on the biochemical profile of urine. J Appl Toxicol 2010;30:354-60.
47. Shinohara N, Matsumoto K, Endoh S, Maru J, Nakanishi J. In vitro and in vivo genotoxicity tests on fullerene C60 nanoparticles. Toxicol Lett 2009;191:289-96.
48. Monteiro-Riviere NA, Linder KE, Inman AO, Saathoff JG, Xia XR, Riviere JE. Lack of hydroxylated fullerene toxicity after intravenous administration to female Sprague-Dawley rats. J Toxicol Environ Health A 2012;75:367-73.

Coffee Break

ナノマテリアルの安全性評価（2）

●大阪大学大学院薬学研究科・薬学部（研究科長・学部長）
大阪大学大学院薬学研究科毒性学分野（教授）
堤 康央

あくまでも仮定の話であることにご留意いただきたいが、例えば、ある日、“ナノマテリアルの安全性に懸念！？”という見出しが、新聞紙上やネットニュースに掲載されたとしよう（空想の世界です）。真偽は横において、いつ新聞に出てもおかしくない見出しである。いや、すでに、似たような見出しは、いくつかの新聞紙上に掲載されているかもしれない。この記事を、薬学的観点からよくよく読んでみると、“普通ではあり得ない限界量まで、あえて曝露”することで、「ハザード」を探索・探求し、この「ハザード」の同定の結果をもとに、個々の最大無毒性量（NOAEL）やADI（一日許容摂取量）の設定を試みた研究の結果であることに気づかされる。いわずもがなではあるが、“あり得ない限界量の曝露”で初めて見られる「ハザード」なので、通常の環境下で生活しているわれわれは、「安全」であり、いわゆる「リスク」は極めて低いことになる。

しかし、これを見た一般の読者（特に、忙しくて見出しのみ閲覧した方）は、どう感じるであろうか？　パニックに陥る人はおられないかもしれないが、“そういえば先日、ナノマテリアルを含んだ化粧品を、購入したばかり…。皮膚は荒れてはいないだろうか？”とか、“このペンキ、よく見るとナノマテリアルが入っているけど、大丈夫？”などと、不安を覚える人、食品・化粧品・衣類など、ナノマテリアル含有製品の購入を控えようとする人は、少なからずおられるのではないだろうか。興味深いことに、「安全である」のに、「安心できない」・「不安である」という状況が生まれることになる。似たような話はいつの時代にもあり、“食品容器から毒性物質”と報道されれば、食品会社の株は暴落するし、“ワインの成分が寿命を延ばす”と報道されれば、ワインが飛ぶように売れる。良いか悪いかはさておいて、特に日本ではこのような風潮が強い傾向にあろう。

そもそも、毒性・安全性を議論する前に、「リスク」と「ハザード」を区別して理解している一般消費者はどの程度いるのであろうか？　おそらく、「ハザード」と聞いても、とあるテレビゲームのことしかイメージできない場合が大半ではなかろうか。物質の「リスク」は、個々それぞれの「ハザード（固有の毒性）」と、時間的・量的に物質に出会う（曝露する）機会の積算によって運命づけられる。簡単な例えでは、コブラの蛇毒の毒性（ハザード）は極めて高い一方で、少なくとも日本で暮らす限り、よほどのことがなければ、コブラと接する機会はなく（コブラ毒を曝露する機会はない）、コブラ毒により死ぬリスクはほぼ0である。また、動物園に行っても、トラやライオンに襲われるリスクが0なのは、檻の中で飼育するという「リスク管理」により、われわれが接触する機会をなくしているためである。このように、「リスク」と「ハザード」は明確に異なるものであるものの、頻繁に、「リスク」と「ハザード」が混同され、「ハザード」だけが一人歩きし、予期せぬ社会現象を生じることがある。特に、冒頭のように、新聞やテレビ、ネットで「ハザード」のみが、あたかも「リスク」と同意義で報道されてしまった場合、「安全」かどうかはさておき、使用者はいわばパニック状態になり、「X社の化粧品や食品はすべて危険！絶対に使用してはダメ！」といった風評被害がたびたび起きている。農薬、食品添加物を含むあらゆる化学物質は、ADI（許容一日摂取量）やTDI（耐容一日摂取量）などの許容量が定められており、どんなに危険な「毒物」であっても、曝露しない、あるいは許容量以下であれば、科学的事実・根拠に基づいて「安全」が確保されているものの、「安心」ではないという典型例ともいえよう。

さて、本題に入るが、ナノマテリアルのリスクはどの程度のものであろうか？　すでに実用化されているナノマテリアルの多くは、製造・販売メーカーがさまざまな毒性評価を実施したうえで、安全性が担保されているものと推察される。一方で、新たな機能を有した「100nm以下のサイズのナノマテリアル」や「10nm以下のサイズのサブナノマテリアル」の開発と実用化が加速し、さらには第3の新素材も近い将来に台頭してこよう。特に、「ものづくり力」に圧倒的な強みを有するわが国においては、この点で、今後も世界をリードしていくもの

と推察される。しかし、ナノマテリアルの有効性・安全性は、素材・大きさ・形状・表面性状・分散／凝集状態などにより大きく異なることなどを鑑みると、いまだ安全性の面で考慮すべき点は多く、適切なリスク評価を推進していく必要があろう。リスク評価においては、曝露経路（吸引〈経鼻・経肺〉・摂取〈経口〉・接触〈経皮〉など）により、どの程度の量が体内に吸収されるのか、吸収された場合には、どこの組織にどの程度分布し、いつ代謝・排泄されるのかといったADME情報を収集することが重要となる。そのうえで、発がん性や生殖発生毒性などのハザード（T）を同定し、どの程度の量なら許容できるのかといった閾値を算出する。これらの解析、所謂、ADMET（動態・毒性）解析を進めることにより、このナノマテリアルは、許容量以下でしか含有されていないので、一生摂取しても大丈夫といった、科学的根拠に基づいた安全性が担保されることになる。今後も続々と開発されるであろうナノマテリアルについて、このような安全性評価が適切になされることを祈るばかりである。そのうえで、先進国、科学技術立国、そして健康長寿立国としてのわが国としては、Medicinal Chemistryにより、物性などを最適化し、有効性を保持した状態で、安全性を担保したものに仕上げていくNano-Safety Design（ナノ最適デザイン）研究が必要不可欠であり、「有用なのは当たり前で、Made in Japanは、しかも安全で安心」という、付加価値を如何に追求していくかが、今後の鍵ではないかと感じている。

一方で、消費者心理として、医薬品に関しては、「リスク」と「ベネフィット」のバランスであり、その「匙加減」次第では、「毒」にも「薬」にもなり得ることを感覚的に理解しつつも、化粧品・食品や、それらに含有される化学物質には、「メリットはあっても、リスクがあるはずがない」という、いわゆる「ゼロリスク」神話が根づいているように感じられる。そのため、たとえハザード情報の報道であったとしても、一旦、「自分の中での安心」が綻びれば、「安全」であるとわかっていても、「不安」が一気に増大し、「安心」を取り戻すことは困難である。そのため、ナノマテリアルの物質的な「安全」と「有用性」の追求はもちろんのこと、ナノマテリアルに対するメンタル面での「興味」や「関心」、「憧れ」とともに、「安心（納得：社会受容）」にどこまで迫ることができるのかがポイントと考えられる。そのためには、開発・製造・販売者といったメーカーのみならず、マスコミを含めて、使用者（ユーザー）とのより適切な「リスクコミュニケーション」が必要不可欠となってこよう。次回は、この「リスクコミュニケーション」と「リスクリテラシー」について議論できればと思っており、多方面からのご意見やお叱りをお願いしたい。

AUTHOR

堤 康央（つつみ やすお）

大阪大学薬学研究科助手、国立医薬品食品衛生研究所大阪支所医薬基盤研究施設 副プロジェクト長、独）医薬基盤研究所 プロジェクトリーダーを経て、2008年 大阪大学大学院薬学研究科毒性学分野 教授（現職）、2012年 大阪大学大学院薬学研究科 研究科長（現職）、大阪大学薬学部薬学部長（現職）

E-mail: ytsutsumi@phs.osaka-u.ac.jp

FOOD SAFETY

doi: 10.14252/foodsafetyfscj.2015005

Review (Invited)

Applications and Safety of Nanomaterials Used in the Food Industry

Kazuma Higashisaka[1,2], Yasuo Yoshioka[1,2,3], Yasuo Tsutsumi[1,4,5]

[1]Laboratory of Toxicology and Safety Science, Graduate School of Pharmaceutical Sciences, Osaka University, 1-6 Yamadaoka, Suita, Osaka 565-0871, Japan
[2]Laboratory of Biopharmaceutical Research, National Institute of Biomedical Innovation, 7-6-8, Saito-Asagi, Ibaraki, Osaka 567-0085, Japan
[3]Vaccine Creation Project, BIKEN Innovative Vaccine Research Alliance Laboratories, Research Institute for Microbial Diseases, Osaka University, 3-1 Yamadaoka, Suita, Osaka 565-0871, Japan
[4]Laboratory of Innovative Antibody Engineering and Design, Center for Drug Innovation and Screening, National Institute of Biomedical Innovation, 7-6-8 Saito-Asagi, Ibaraki, Osaka 567-0085, Japan
[5]The Center for Advanced Medical Engineering and Informatics, Osaka University, 1-6, Yamadaoka, Suita, Osaka 565-0871, Japan

A survey by the United States Food and Drug Administration (USFDA), in 2008, has revealed that more than 80 nanomaterial-containing food and drink items were available for consumption around the world at that time, and estimated that the Japanese market for nanomaterial-containing food could reach 250 billion yen in 2030. Potential uses of nanotechnology have been identified in almost all segments of the industry, including the following four key areas: agriculture, nutritional supplements and nutraceuticals, food processing, and food packaging. Despite a rapid development of its use in the food sector, little is known about the *in vivo* and *in vitro* kinetics of nanomaterials. Consequently, the risks of nanomaterials have not been analyzed. Nanoparticles are reported to be absorbed across the intestinal barrier via transcellular, paracellular, and junctional pathways, but the bioavailability of each material may be different due to different effects of various factors. Questions about these compounds already raised safety concerns, although the history of their use in the food sector is yet short. In this review, we overview the currently available information regarding the safety of the three main nanomaterials used in the food industry to provide the scientific basis for the risk assessments that are necessary for the development and safe use of nanomaterials in the food sector.

Key words: food sector, nanomaterial-containing foods, nanotechnology, safety concern

1. Introduction

Recent innovations in science and technology, as well as their globalization, have brought sweeping changes to people's eating habits. The number and diversity of chemicals in our food, such as additives, agricultural chemical residues, contaminants, as well as new materials and ingredients to maintain or improve health or prevent lifestyle-related diseases, have increased rapidly. We ingest such chemicals throughout our lifetime often without being aware of them.

Received: 31 January 2015; Accepted: 9 June 2015; Published online: 29 June 2015
* Corresponding author: Yasuo Tsutsumi; ytsutsumi@phs.osaka-u.ac.jp
The contents of this article reflect solely the view of the author(s).
Abbreviations: ADI, acceptable daily intake; EFSA, European Food Safety Authority; USFDA, United States Food and Drug Administration

Because consumer's interests in food safety concerns are increasing, the safety assessment of these chemicals in our food is essential.

Nanomaterials may offer particular cause for concern due to their small size imparting their unique properties. Nanomaterials with diameters of ≤100 nm are currently used in various applications, including food production (for example, to improve food texture). As the size of particles decreases, their specific surface area increases, and the high specific surface area of nanomaterials results in a dramatic increase in surface coverage and water absorbability compared with those of materials with diameters of >100 nm.

In 2015, a consumer products inventory compiled by the Woodrow Wilson International Center for Scholars listed 117 nanomaterial-containing products in the food and beverage category, which includes foods, beverages, and cooking items[1]. It was estimated that the Japanese market for nanomaterial-containing food could reach 250 billion yen in 2030[2]. With the expansion of this market, the likelihood of human exposure to nanoparticles via the intestinal tract will increase. Even though the amounts of nanomaterials present in food are small, they will tend to be consumed over a long period of time, and therefore it is necessary that biological responses to oral ingestion of nanomaterials be assessed and that information about exposure levels be provided. Although there have been a few studies on the biological effects of nanomaterials on humans, and unexpected biological responses to nanomaterials have recently been reported[3,4], the safety of nanomaterials has not been thoroughly assessed. Little is known about their *in vivo* and *in vitro* kinetics at biologically relevant concentrations via different administration routes. In general, chemical risk analysis involves the integration of hazard information and information about absorption, distribution, metabolism, and excretion for the actual exposure route. Nanomaterials, including those contained in foods, are no exception. Owing to the size of nanomaterials that is the same order of magnitude as that of viruses, their toxicokinetics *in vivo* is unpredictable. In addition, the fact that they can penetrate the intestinal barrier and be absorbed into cells must be considered in evaluations of their *in vivo* kinetics.

The aim of this review is to describe the current uses of nanomaterials in the food sector and summarize an overview of the available data on the safety of nanomaterials.

2. Nanotechnologies in the Food Sector

From many reports and reviews on the current and short-term projected applications of nanotechnologies in the food industry, their potential uses are found for almost all segments of the industry[4,5].

Nanotechnologies have been successfully applied to agri-food production, as has been focused by several key reports[6,7]. Application of nanotechnologies in this food sector has begun to grow now since it has been recognized that conventional agricultural techniques cannot further increase productivity or restore damaged ecosystems[6]. New tools were developed also for nanobiosensing applications[7] which can be used for sensing a wide variety of fertilizers and pesticides, as well as moisture. These are expected to be useful for the identification of crop diseases and agrochemical residues[7], the augmentation of agricultural productivity through genetic improvements of plants[8], and the improvement of the ability of plants to absorb nutrients[9]. Consumer's demand for healthy foods has encouraged researchers to apply nanotechnology to food and nutrition. For instance, nanomaterials have been used to coat food packaging, and nanosieves are used to filter out microorganism and even viruses. In addition, the development of analytical methods for assessment of nanotechnology has been remarkable[10,11]. Moreover, application of nanotechnology in the food and nutrition sector has resulted in the development of food ingredients with increased functionality such as improved physical or chemical properties and physiological performance[12].

Such ingredients are widely used to improve the taste and nutritional value of food products and to prolong shelf-life. Many food products containing engineered nanomaterials are now widely available; for example, titanium dioxide and silica nanoparticles are used as food additives[5]. The strong antimicrobial properties of chitosan[13], silver nanoparticles[14], and photocatalytic titanium dioxide[15] have also been exploited in the food sector. In addition, nano-encapsulation technologies are being used for the development of artificial colorants, preservatives, and aroma compounds. These technologies hopefully will make it possible to disperse or solubilize materials that are otherwise poorly soluble in water, to improve the efficacy of additives, and to improve the absorption rate of encapsulated supplements and nutrients.

Food-packaging materials represent the largest category of applications of nanotechnology in the food sector[16]. Containers and wrapping materials that come into direct contact with food contain nanomaterials to improve packaging properties, such as gas impermeability[17] and against temperature and moisture[18]. Nanomaterials can also impart antibacterial activity or carry out deoxygenation reactions. Containers and wrapping materials containing nanosensors,

referred to as intelligent food packaging, have been used to detect the condition of food inside packaging[19]. In Europe, carbon black and silica dioxide nanomaterials have been already used as food contact materials.

3. Behavior of Ingested Nanomaterials

We are intentionally and unintentionally exposed to various substances through dermal, intraoral, and pulmonary routes; and oral absorption is the major route by which we take in chemicals, as well as nutrients and water. Given that nanoparticles are now included in various food products, it is assumed that the digestive organs, including the intestinal tract, are exposed to nanoparticles daily. Nanoparticles ingested orally travel from the mouth to the stomach and intestines. The epithelial cells lining the small intestine absorb most nutrients, as well as nanomaterials, by endocytosis or by diffusion and transport them across the epithelium. As nanoparticles move through the small intestine, they come into contact with intestinal epithelial cells.

Absorption of nanoparticles has been studied using Caco-2 cell monolayers as gut models. These studies have shown that nanoparticles are transported from the luminal side to the basal luminal side of intestinal epithelial cells, probably by endocytosis or transcytosis[20–22]. Several pathways are available for the absorption of particles across intestinal barriers (**Figure 1**). The transcellular route is the most relevant to the uptake of nanomaterials[23] because the tight junctions of epithelial cells eliminate macromolecules[24]. The size limit of the paracellular route, which depends on the animal species and the tissue examined, has been variously reported as being from 0.6 to 5 nm[25]. Some nanomaterials, such as chitosan nanoparticles, were reported to be able to loosen epithelial tight junctions, suggesting that these nanoparticles may promote the paracellular transport of macromolecules[26,27].

Microparticles (>100 nm) in the gut are absorbed mainly through M-cells[28]. M-cells are present in the epithelium of mucosa-associated lymphoid tissues and can transport macromolecules and particles in the gut lumen into cells of

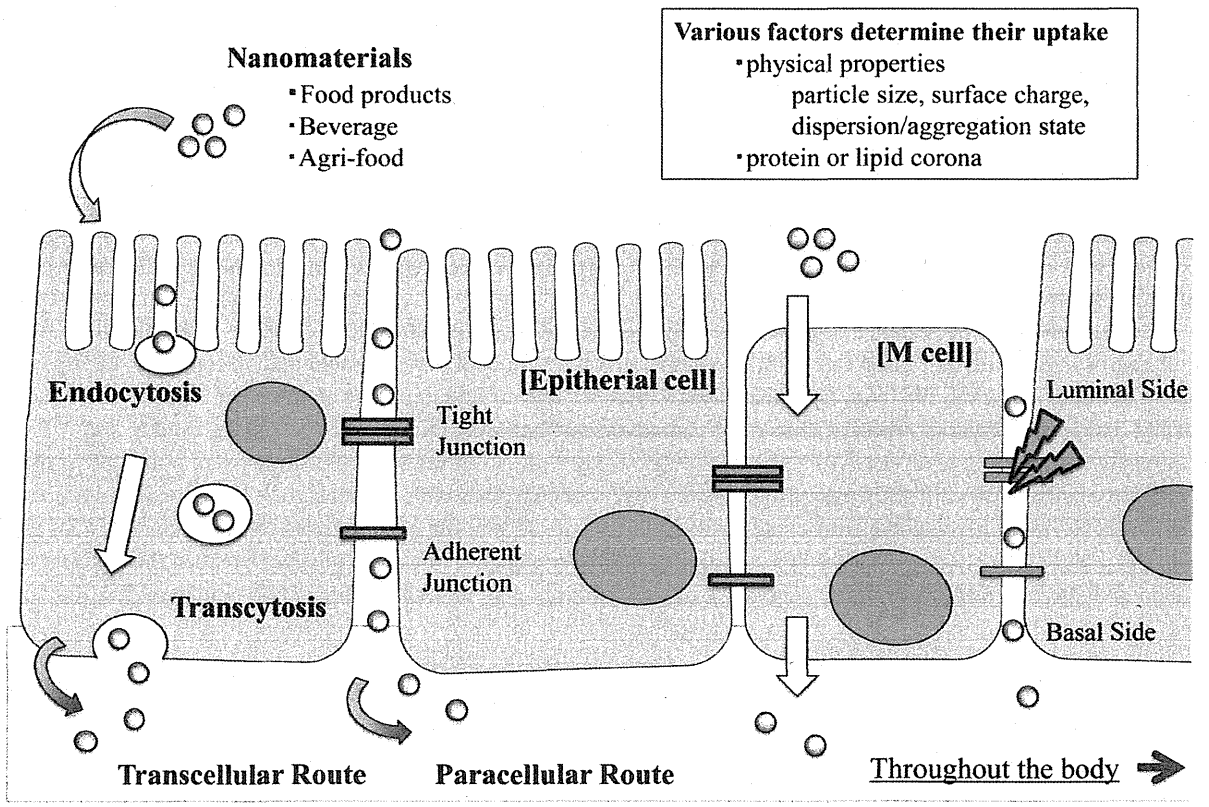

Fig. 1. The various absorption route of particles across intestinal barriers.

the immune system[29,30]. It is generally believed that nanoparticles in the intestine are taken up by enterocytes and goblet cells as well as by M-cells in the Peyer's patches and the isolated follicles of the intestinal-associated lymphoid tissue[31,32]. In fact, Brun et al reported that translocation of titanium dioxide nanoparticles through the regular ileum epithelium at Peyer's patches can induce epithelium impairment[33]. Therefore, it is reasonable to assume that nanoparticles can be absorbed through epithelial cells.

Cellular uptake of nanoparticles depends on their physical properties, such as particle size, surface charge, and dispersion or aggregation state[34,35]. To clarify a major role of surface properties in the extent of intestinal absorption of silica nanoparticles, we used an everted gut sac model where intestinal sacs from rats were incubated in solutions containing silica particles. Using inductively coupled plasma optical emission spectrometry, we found that silica nanoparticles modified with a carboxyl group or an amino group was more readily absorbed from the mucosal side to the serosal side of the sacs than were unmodified nanoparticles[36]. Schleh et al studied how the physical properties of gold nanoparticles affected the amount of the nanoparticles that passed through the intestinal membranes in adult female rats treated with gold nanoparticles of five different sizes (1.4–200 nm) and opposite surface charges. They revealed that absorption across the intestinal barrier decreased with increasing particle size and that negatively charged particles (2.8 nm) were more readily absorbed than positively charged particles (2.8 nm)[37]. Various factors have been suggested to affect intracellular transitivity of nanomaterials. The formation of a protein corona or lipid corona on the surface of nanomaterials may change their interaction with various receptors expressed on the surface of cells[38,39]. Specifically, the formation of a protein corona alters the physicochemical characteristics of nanoparticles, such as size and interfacial composition, which can in turn impart new biological characteristics to the nanomaterials and change their effects on cells exposed to them.

4. Types of Nanomaterials Used in Food and Evaluation of Their Safety

The major nanomaterials used in consumer products are silver, silica, and titanium dioxide. Among different product categories, silver nanomaterials are the most widely used, and particularly common in products in the food and beverage category and the home and garden category[40,41].

4.1. Applications and Safety of Silver Nanoparticles Used in the Food Industry

Owing to the antimicrobial activity of silver, silver nanoparticles are widely used in consumer products[14,42]. The mechanism of the antibacterial activity of silver nanoparticles has not been elucidated, but they may interact with the membranes of bacteria. The antibacterial activity of silver nanoparticles is likely due in part to Ag^+ ions readily formed on the surface of the nanoparticles through the reaction with oxygen, and the antibacterial activity of silver nanoparticles increases with decreasing particle size, which has been attributed to the increase in the surface area to mass ratio as particle size decreases[43].

Growing amounts of evidence suggest that orally ingested silver nanoparticles can cross the gastrointestinal barrier, be absorbed into the blood[44], and cause adverse health effects. Kim et al demonstrated that 56-nm silver nanoparticles can be found in rat blood, the liver, and other organs after 90 days of oral exposure at a dose of 30, 125, or 500 mg/kg bw/day. These investigators reported a no-observed-adverse-effect level (NOAEL) of 30 mg/kg bw/day and a lowest-observed-adverse-effect level (LOAEL) of 125 mg/kg bw/day[45]. It is reported that when rats were orally administered for 28 consecutive days with suspensions of uncoated silver nanoparticles with diameters of <20 nm or with suspensions of polyvinylpyrrolidone-coated nanoparticles with diameters of <15 nm, the nanoparticles were distributed in all the organs, but mainly in the liver[44,46]. Based on comparisons of the organ concentrations of silver between the nanoparticles-treated and silver nitrate-treated rats, they suggested that mainly Ag^+ ion, rather than silver nanoparticles, passed the intestines of rats[45]. In another study in rats, localization of silver in the liver was detected in several cell types, such as Kupffer cells and sinusoidal endothelium cells[45,47]. However, Van der Zande et al reported that in rats exposed to silver nanoparticles for 28 days, plasma levels of alanine aminotransferase and aspartate transaminase were relatively low compared with control values and that there were no significant differences between the silver-treated groups and the respective control groups. These investigators suggested that the silver nanoparticles induced no acute hepatotoxicity[44].